

# National Report of Poland to EUREF 2018

J. Krynski

Institute of Geodesy and Cartography, 27 Jacka Kaczmarskiego St., 02-679 Warsaw

E-mail: krynski@igik.edu.pl

J.B. Rogowski

Gdynia Maritime University, 81-87 Morska St., 81-225 Gdynia

E-mail: jerzyrogowski@gmail.com

## 1. Introduction

Since 2016 the main geodetic activities at the national level in Poland concentrated on maintenance of monitoring the terrestrial reference frame, gravity control and geomagnetic control, continuing operational work of permanent IGS/EPN GNSS stations, GNSS data processing on the regular basis at the WUT and MUT Local Analysis Centres, activities of MUT and WUT EPN Combination Centre, activity within the EUREF-IP Project, works on GNSS for meteorology, monitoring ionosphere and ionospheric storms, advanced methods for satellite positioning, maintaining the ASG-EUPOS network in Poland, modelling precise geoid, the use of data from satellite gravity missions, monitoring gravity changes, geodynamics, activity in satellite laser ranging and their use.

## 2. Monitoring the terrestrial reference frame

Research on monitoring the terrestrial reference frame was conducted at the Faculty of Civil and Environmental Engineering of the Gdansk University of Technology (GUT). The impact of ITRF2014/IGS14 on the positions of the reference stations in Europe was investigated (Figurski and Nykiel, 2017).

ITRF2014 – a new realization of the ITRS introduced in January 2017 exhibits high consistency with the previous ITRF2008 solution. However, the introduction of the new satellite and ground antennas phase centre calibrations in IGS14 leads to non-negligible differences in station positions. The updated antenna phase centre models cause a change in the scale of the network at the level of 0.7 ppb. Also the translation parameters are changed, for all translation components, while the network orientation remains unchanged. Scale changes cause changes in baselines length between the stations (in most cases the increase of length was observed). It was shown that the variable number of fixed reference stations in the GNSS local networks affects only the translation of the frame, and the change of its parameters is correlated with the number of fixed reference stations.

Differences between ITRF2008 and ITRF2014 were confirmed to be minor. However, changing GNSS antenna calibrations from IGB08 to IGS14 causes changes of stations coordinates up to several millimetres, especially for the vertical component. This effect is mainly due to the introduction of new or updated absolute antenna calibrations. Such changes of coordinates have also impact on the realization of the ETRF. Coordinate time series for POTS00DEU and DARE00GBR stations, which antennas have been changed between IGS08.atx and IGS14.atx illustrate an impact of a new reference frame and improved antenna models on the stability of EPN stations. At POTS00DEU the individual calibration was introduced (instead of type mean) and at POTS00DEU, the improved type mean calibration was presented. The coordinates of those stations were estimated in IGB08 frame with IGS08 antennas calibrations (dotted line in Fig. 1) from 1928 to 1933 GPS week and in IGS14 frame with IGS14 antennas calibrations (solid line in Fig. 1) from 1928 to 1937 GPS week.

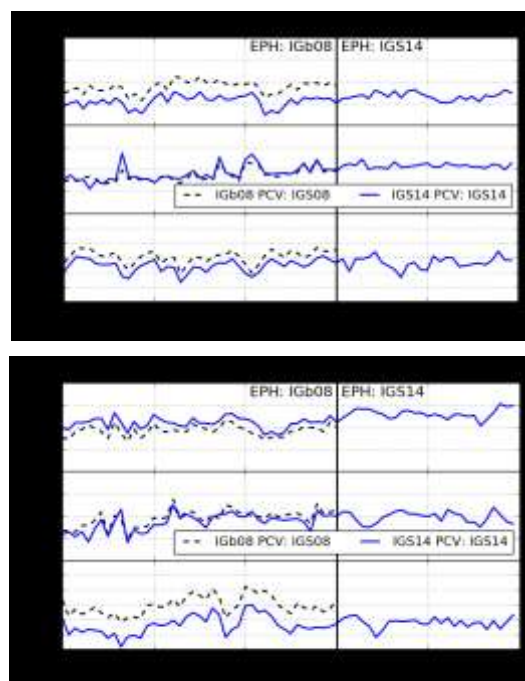


Fig. 1. Positioning results (w.r.t. IGB08 EPN cumulative solution at 1934 GPS week) for POTS00DEU (Potsdam, Germany) and DARE00GBR (Daresbury, UK) stations

Calculations were performed using the Bernese double difference GNSS processing, which assumes the use of constrained stations and fixed satellite ephemeris to estimate positions in ITRFyy. This becomes a problem when the impact of different phase centre calibration on position is investigated. Further research should concern the elaboration of the network using the PPP method (if obtained accuracy will be at the level of differential method), in which the reference frame is transferred to the points using only satellite ephemeris. Only in this way the quantitative and qualitative influence of the new IGS14 antenna calibration on the implementation of ITRF2008 in Europe can be investigated (Figurski and Nykiel, 2017). However, the results obtained showed that the only method that will effectively remove the discontinuities caused by the new antenna calibrations is the third reprocessing of archived GNSS observations.

### 3. Current status of reference frames in Poland

#### 3.1. Horizontal and vertical

In 2017, the Head Office of Geodesy and Cartography continued field inspection of geodetic control network. About 50% of geodetic control stations was already visited.

#### 3.2. Vertical

The Head Office of Geodesy and Cartography initiated in 2017 preparations for a new levelling campaign in Poland. Following the existing regulations the campaign is planned to start around 2020. Major advantages of combining levelling networks with state-of-the-art GNSS measurements and gravity field models in Poland are noted.

The PL-EVRF2007-NH is in the process of being implemented by local authorities. According to Polish regulations, the EVRF2007 solution should be implemented locally by the end of 2019, at latest.

#### 3.3. Gravity

Research activities concerning gravity field modelling and gravimetric works performed in Poland in 2017 focused on geoid modelling, evaluation of global geopotential models, determination of temporal variations of the gravity field with the use of data from satellite gravity space missions, absolute gravity surveys for the maintenance and modernization of the gravity control, analysis of first results of the superconducting gravimeter at the Borowa Gora Geodetic-Geophysical Observatory, metrological aspects in gravimetry, and investigations of the non-tidal gravity changes.

### Maintenance of gravity control and gravity survey for geodynamic research

Absolute gravity measurements were carried out on regular basis with the use of regularly compared with other absolute gravimeters (e.g. Pálinkáš et al., 2017) FG5-230 gravimeter in the Jozefoslaw Astrogeodetic Observatory of the Warsaw University of Technology (WUT) since 2005 (Fig. 2). Ground water level was recorded by hydrostatic piezometer and five soil moisture sensors from 0.5 m to 6.0 m depth (Krynski and Rogowski, 2017).

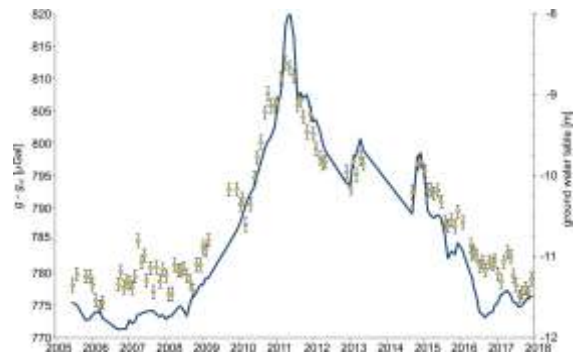


Fig. 2. Absolute gravity surveyed with the FG5-230 at Jozefoslaw (100 cm height) ( $g_{ref} = 981213000 \mu\text{Gal}$ )

In 2017 also pluviometer as well as solar radiation sensor were installed in the Observatory. Changes of gravity due to hydrological variations at the Jozefoslaw Astrogeodetic Observatory were investigated (Olszak et al., 2017)

Gravimetric investigations at the Borowa Gora Geodetic-Geophysical Observatory of the Institute of Geodesy and Cartography (IGiK) were continued. A series of absolute gravity measurements on the test stations in the Observatory, conducted on monthly basis with the A10-020 gravimeter since September 2008 (Fig. 3), shows high quality of A10 gravimeter results.

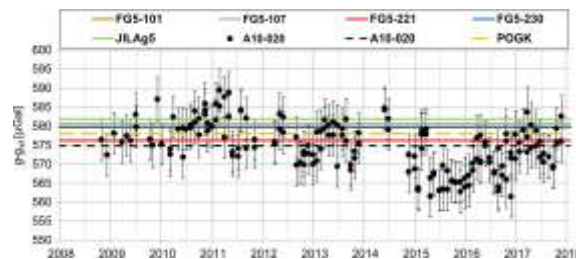


Fig. 3. Absolute gravity surveyed with the A10-020 at A-BG station in Borowa Gora (pillar level) ( $g_{ref} = 981250000 \mu\text{Gal}$ )

Starting from late 2014, regular measurements with the A10-020 gravimeter at three sites in Borowa Gora Geodetic-Geophysical Observatory are supplemented with the monitoring of local hydrological conditions via automated stations measuring precipitation, soil humidity (at two depths 0.1 m and 0.5 m) and water table level

variation. Local hydrological model was developed (Dykowski and Krynski, 2017). Sensitivity of the A10 absolute gravimeter to the variation of local hydrological conditions allowing to detect small local hydrological changes was demonstrated (Fig. 4). It has also been proven that MERRA hydrological model is efficient for hydrological variations analysis.

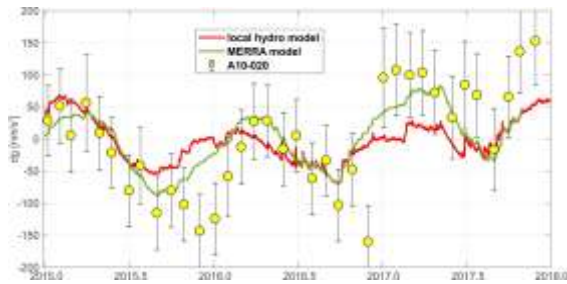


Fig. 4. Absolute gravity variations from the survey with the A10-020 at the field station 156 at Borowa Gora and from local as well as MERRA hydrological models

Since May 2016 the iGrav-027 superconducting gravimeter operates at the Borowa Gora Geodetic-Geophysical Observatory. First year of gravity signal records with the iGrav-027 was summarized and reported (Dykowski et al., 2017b). Tidal adjustment confirms the expected performance of the iGrav-027 at sub  $\text{nm/s}^2$  level. Atmospheric and hydrological models prove to be a very useful tool in the analysis of time series of gravity variation. It was shown that local hydrological model needs evaluation of the umbrella effect as well as the location of the iGrav-027 sensor below ground level.

The drift of the iGrav-027 was determined by comparison of its record with the with gravity determinations using the A10-020 absolute gravimeter at the site collocated with that of the superconducting gravimeter. Differences obtained with fitted exponential functions are shown in Figure 5

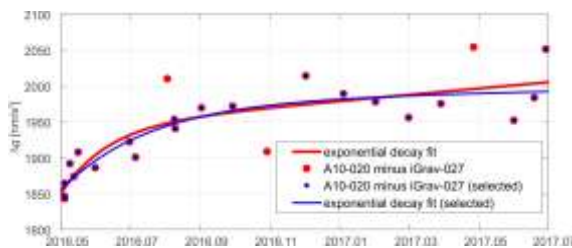


Fig. 5. Differences between the records of the iGrav-027 superconducting gravimeter and gravity determined with the A10-020 absolute gravimeter together with fitted exponential functions

The calibration of the iGrav-027 sensor was carried out from 19 to 29 May 2017 with the use of three LCR G gravimeters as well as the A10-020, within the period of the timewise nearest highest

amplitude of tidal curve (summer tide) for the Borowa Gora Observatory (Fig. 6).

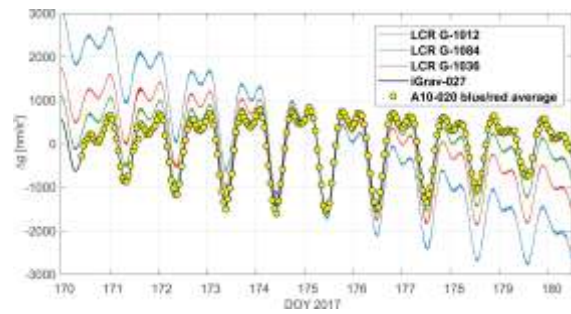


Fig. 6. Raw data from all relative gravimeters and the A10-020 absolute gravimeter used for calibration of the iGrav-027

The iGrav-027 superconducting gravimeter is a valuable tool for controlling the national gravity standard. Borowa Gora Observatory with three suitable pillars, equipped with the iGrav-027 and the A10-020 absolute gravimeter can successfully serve as a site for regional comparisons of absolute gravimeters. As the A10-020 is a regular participant of the international comparison campaigns of absolute gravimeters (e.g. Pálinkáš et al., 2017) and the iGrav-027 superconducting gravimeter is operational, Borowa Gora Observatory qualifies to be an important component of the new definition of gravity reference system as a station with a continuous gravity reference function.

### 3.4. Magnetic

Magnetic control in Poland, consisting of 19 magnetic repeat stations maintained by IGiK is supported by two magnetic observatories run by the Institute of Geophysics of the Polish Academy of Sciences (IGF PAS): Central Geophysical Observatory in Belsk and Magnetic Observatory in Hel. In addition, there are two permanent magnetic stations: Borowa Gora – run by IGiK, and Suwalki – run by IGF PAS

Measurements of three independent components of the magnetic intensity vector, i.e. declination ( $D$ ), inclination ( $I$ ) and the module of the magnetic intensity vector ( $F$ ) were performed in 2017 at 17 repeat stations of the fundamental magnetic control as well as at 8 densification stations (Fig. 7).

The coordinates of the magnetic repeat stations were determined in the PL-ETRF2000 reference frame, and normal heights in the PL-KRON86 frame. The magnetic data acquired were included into the state database PRPOG of geodetic, gravimetric and magnetic control data.

The need for the establishment of the magnetic repeat stations on the Baltic Sea was investigated (Welker et al., 2017).

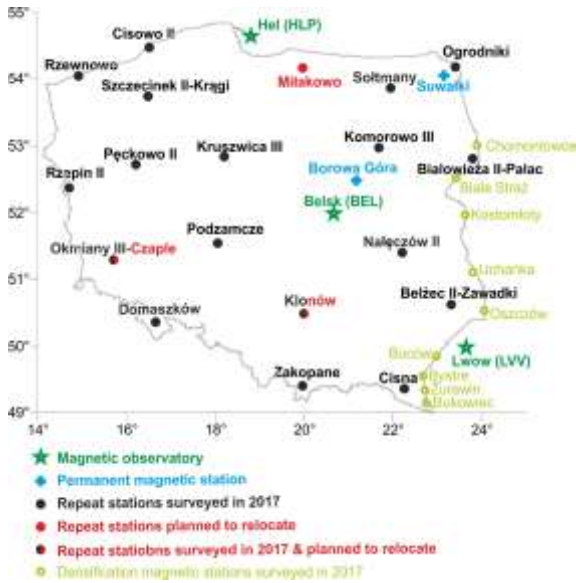


Fig. 7. Magnetic stations surveyed in 2017 and magnetic observatories

#### 4. Participation in IGS/EPN permanent GNSS networks

##### 4.1. Operational work of permanent IGS/EPN stations

Permanent IGS and EPN GNSS stations operate in Poland since 1993. Recently 18 permanent GNSS stations (Table 1), i.e. Biala Podlaska (BPD), Borowa Gora (BOGO, BOGI), Borowiec (BOR1), Bydgoszcz (BYDG), Gorzow Wielkopolski (GWWL), Jozefoslaw (JOZE, JOZ2), Krakow (KRAW, KRA1), Lamkowko (LAMA), Lodz (LODZ), Katowice (KATO), Redzikowo REDZ (Suwalki (SWKI), Ustrzyki Dolne (USD), Wroclaw (WROC) and Zywiec (ZYWI) (Fig. 8) operate in Poland within the EUREF program. The stations BOGI, BOR1, JOZE, JOZ2, LAMA and WROC operate also within the IGS network ([http://www.epncb.oma.be/\\_networkdata/stationlist.php](http://www.epncb.oma.be/_networkdata/stationlist.php)). A brief characteristics of those stations is given in Table 1. Data from those stations are transferred via internet to the Local Data Bank for Central Europe at Graz, Austria and to the Regional Data Bank at Frankfurt/Main, Germany and together with data from other corresponding stations in Europe, were the basis of the products that are applied for both research and practical use in geodesy, surveying, precise navigation, environmental projects, etc.

Four of those stations, i.e. BOGI, BOR1, JOZ2 and WROC participated also in IGS Real-time GNSS Data project. Two stations WROC and BOR1 are also included into the IGS Multi-GNSS Experiment (MGEX) pilot project (<http://igs.org/mgex>).



Fig. 8. EPN/IGS permanent GNSS stations in Poland (2017)

The EPN stations at Borowa Gora (BOGI), Borowiec (BOR1), Jozefoslaw (JOZ2, JOZ3), Cracow (KRAW, KRA1), Lamkowko (LAMA), and Wroclaw (WROC) take part in the EUREF-IP project ([http://igs.bkg.bund.de/root\\_ftp/NTRIP/streams/streamlist\\_euref-ip.htm](http://igs.bkg.bund.de/root_ftp/NTRIP/streams/streamlist_euref-ip.htm)) (Fig. 9).

Since March 2005 Ntrip Broadcaster is installed at the AGH University of Science and Technology (<http://home.agh.edu.pl/~kraw/ntrip.php>). Ntrip Caster broadcasts RTCM and raw GNSS data from KRAW0 and KRA10 sources take part in the EUREF-IP project and provide data to regional EUREF broadcasters at BKG, ASI and ROB.



Fig. 9. Polish EPN stations participating in the EUREF-IP project (2017)

Table 1. Permanent GNSS stations in Poland

| Name (abbreviation)        | Latitude  | Longitude | Status     |
|----------------------------|-----------|-----------|------------|
| Biala Podlaska (BPDL)      | 52°02'07" | 23°07'38" | EUREF      |
| Borowa Gora (BOGI)         | 52°28'30" | 21°02'07" | IGS, EUREF |
| Borowa Gora (BOGO)         | 52°28'33" | 21°02'07" | EUREF      |
| Borowiec (BOR1)            | 52°16'37" | 17°04'24" | IGS, EUREF |
| Bydgoszcz (BYDG)           | 53°08'04" | 17°59'37" | EUREF      |
| Gorzow Wielkopolski (GWWL) | 52°44'17" | 15°12'19" | EUREF      |
| Jozefoslaw (JOZE)          | 52°05'50" | 21°01'54" | IGS, EUREF |
| Jozefoslaw (JOZ2)          | 52°05'52" | 21°01'56" | IGS, EUREF |
| Katowice (KATO)            | 50°15'11" | 19°02'08" | EUREF      |
| Krakow (KRAW)              | 50°03'58" | 19°55'14" | EUREF      |
| Krakow (KRA1)              | 50°03'58" | 19°55'14" | EUREF      |
| Lamkowko (LAMA)            | 53°53'33" | 20°40'12" | IGS, EUREF |
| Lodz (LODZ)                | 51°46'43" | 19°27'34" | EUREF      |
| Redzikowo (REDZ)           | 54°28'21" | 17°07'03" | EUREF      |
| Suwalki (SWKI)             | 54°05'55" | 22°55'42" | EUREF      |
| Ustrzyki Dolne (USDL)      | 49°25'58" | 22°35'09" | EUREF      |
| Wroclaw (WROC)             | 51°06'47" | 17°03'43" | IGS, EUREF |
| Zywiec (ZYWI)              | 49°41'12" | 19°12'21" | EUREF      |

#### 4.2. Data processing at WUT LAC

The Warsaw University of Technology operates the WUT EPN Local Analysis Centre (LAC) since 1996. WUT AC contributes to EUREF with final (weekly and daily) and rapid daily solutions of the EPN subnetwork (Liwosz, 2015). At the end of 2017, the WUT LAC subnetwork (Fig. 10) consisted of 119 GNSS stations (13 new stations were added in 2017) from which 94% observed both GPS and GLONASS satellites.

GNSS data are processed in WUT LAC using the Bernese GNSS Software v.5.2. In 2017 WUT switched the reference framework from IGB08/epn\_08.atx to IGS14/epn\_14.atx for GNSS data analysis. WUT LAC products, i.e., daily and weekly coordinates in SINEX format and zenith tropospheric delays, can be accessed from the following EPN data centres: BKG (<ftp://igs.bkg.bund.de/EUREF/products>) and EPN (<ftp.epncb.oma.be/epncb/product/clusters>).



Fig. 10. EPN stations providing data processed at WUT EUREF LAC (16 April 2018) (<http://www.epncb.oma.be/>)

#### 4.3. Data processing at MUT LAC

The Military University of Technology in Warsaw (MUT) LAC Analysis Centre provides final (daily and weekly) and rapid solutions processing data from 142 EPN stations (Fig. 11) distributed homogeneously over Europe.



Fig. 11. EPN stations providing data processed at MUT EUREF LAC (16 April 2018) (<http://www.epncb.oma.be/>)

Since GPS week 1798, 8 stations (ARJ6, JON6, NOR7, OVE6, SVE6, UME6, VIL6, VIS6), since GPS week 1812, 3 stations (LEK8, OST6, SKE8), and since GPS week 1940, 4 stations (KEV2, KILP, KIV2, MET2) were added to MUT subnetwork. The last update of the processing strategy took place in 2017 (GPS week 1980). Since then, GAMIT/Globk v.10.61 software is used in MUT AC to process GNSS data.

MUT processes also local GNSS data and provides the station monitoring service. The latest release uses the observations from over 400 permanent stations located in Poland and neighbouring countries. Four GNSS networks are monitored: national ASG-EUPOS and three private networks VRSnet.pl, SmartNet Poland, and TPI NetPro (Fig. 12).



Fig. 12. GNSS networks monitored at MUT

Since 2017 MUT began processing all data in a common way with a joint adjustment to ensure the consistent and unified reference frame in the EPOS programme. Currently, the results of analyses, available with approximately 20-hour delay, can be followed on a dedicated website ([http://www.cgs.wat.edu.pl/gnss/mut\\_gnssr.html](http://www.cgs.wat.edu.pl/gnss/mut_gnssr.html)).

#### 4.4. Activities of MUT and WUT EPN Combination Centre

In 2017, the EPN Analysis Combination Centre (ACC) continued to combine GNSS coordinate solutions provided in SINEX format by 16 EPN Analysis Centres into official EPN solutions.

Since 29 January 2017 (GPS week 1934), the EPN ACs started to use the IGS14/epn\_14.atx framework during GNSS data analysis, to be consistent with IGS products. Since the week 1934, also all EPN combined coordinate solutions are aligned to the latest IGS reference frame – IGS14 (Liwosz i Araszkiewicz, 2017).

At the AC workshop, held in Brussels (25–26 October 2017), it was agreed to harmonize the troposphere modelling among ACs in order to increase the consistency between AC coordinate solutions (9 ACs used VMF1/ECMWF, and 7 used GMF/GPT approach). Since the week 1980 (17–23 December 2017) it is mandatory for all EPN ACs to use the VMF1/ECMWF approach. That approach, with the use of VMF1 forecast grids, was also recommended for rapid analysis. At the workshop, it was also recommended that more ACs will start submitting rapid products, so that all EPN stations could be processed and monitored.

The EPN ACC website (<http://www.epnacc.wat.edu.pl>) was updated in 2017 because of the change in the combination strategy for creating EPN weekly combined solutions. Since November 2016 the EPN weekly combined solutions are based on daily combined solutions (EPN LAC mail 2134). The EPN ACC website contains now graphs and maps presenting coordinate consistency of AC daily solutions with respect to daily combined solutions for each station and day of the last combined week.

#### 4.5. Other EPN and IGS activities

##### *GNSS for meteorology*

Research on assessing areological techniques of water vapour retrieval in one point (at Central Geophysical Observatory, Belsk, Central Poland) was conducted in 2017 in the Warsaw University of Technology (Kruczyk et al., 2017). Three independent techniques used to obtain Integrated Precipitable Water (IPW), i.e. GPS solution, radiosounding and CIMEL sunphotometer, were tested. Semi-permanent GPS station has been set up on the roof of the building of the Central Geophysical Observatory of the Institute of Geophysics PAS in Belsk achieving perfect CIMEL-GPS co-location. Several GPS solutions have been tested including network solutions (subset of EPN network), and PPP solution by automatic CSRS-PPP (V1.05) PPP-On-Line Positioning Service by the webpage of NRCan (National Resources of Canada). CIMEL sunphotometer IPW and IPW values derived from GPS solutions show very good agreement (biases at

the level of 1%). IPW differences show distinct seasonal pattern which is more complicated than a simple periodic term. There is a clear correlation of IPW bias and local atmospheric temperature (Fig. 13) what signals some systematic deficiencies in solar photometry as IPW retrieval technique.

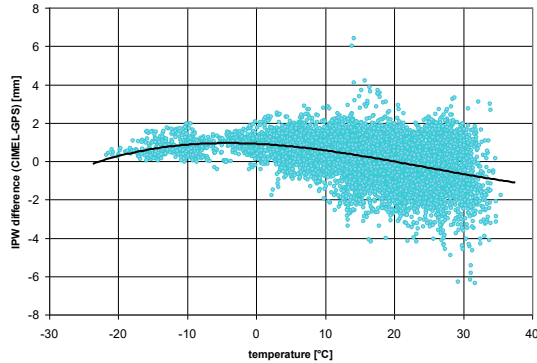


Fig. 13. IPW difference [mm] CIMEL-318 – GPS (PPP solution) for Belsk as a function of atmospheric temperature in 2010-2012 (5 minute interval) with a trend line (8592 points)

Probable cause of this phenomena is a change of optical filter characteristics in sunphotometer or indirect nature of GPS IPW (mapping functions and GPS solutions minutiae).

MUT in cooperation with the Gdansk University of Technology conducted research on the use of GNSS data to sense the dynamics of the atmosphere. The influence of adopted GNSS processing strategy on the long-term ZTD (Zenith Total Delay) parameters was investigated. Eight re-processings of observations from selected EPN stations were conducted, in order to obtain ZTD time series which differ from each other in terms of elevation mask, mapping function, source of ZHD a priori value or software applied. All ZTD solutions obtained were converted to the IWV time series and then the spectral (Lomb-Scargle periodograms) and linear (LSE) analysis of them were performed. Both seasonal and long-term changes determined were compared to each other and validated using in situ measurements from radiosounding (RS) stations (Fig. 14).

The influence of multi-GNSS constellations on the GNSS troposphere products was also investigated. The study was based on only one year of data, and therefore only short-time changes were detected. The ZTDs were calculated with using only GPS satellites, only Galileo satellites, as well as GPS and GLONASS satellites, GPS and Galileo satellites, and finally GPS, GLONASS and Galileo satellites. The mean ZTD bias calculated w.r.t. official EPN solutions (Fig. 15), standard deviations and gradients were analysed. The influence of individual antenna calibration was also investigated.

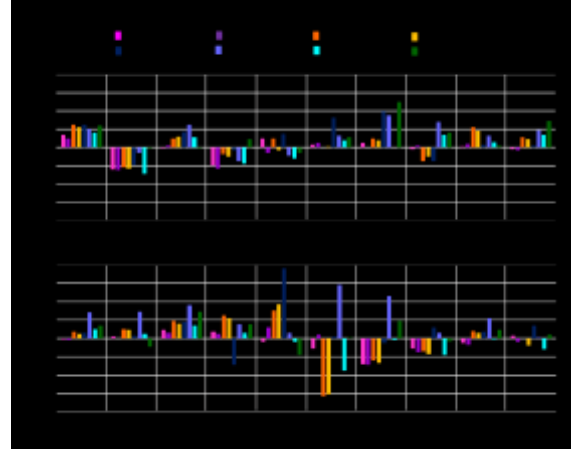


Fig. 14. Differences in IWV linear trend value between analysed GNSS solutions and RS



Fig. 15. Mean ZTD bias (w.r.t. the reference solution) for analysed EPN stations and various constellations (10.2016 – 01.2017 time span)

Research on the impact of Galileo observations on tropospheric parameters and tropospheric gradients was conducted at the GUT (Baldysz et al., 2017). Results of five combinations: GPS-only, Galileo-only, GPS/ Galileo, GPS/GLONASS, and GPS/GLONASS/ Galileo, for the two periods of time, which covered one year (02.2016 – 02.2017) and nearly EOC (10.2016 – 02.2017) time span were analysed and compared with the combined, official EPN product. It was shown that after EOC, the addition of Galileo observations to the e.g. GPS observations caused slightly improvements in obtained ZTD values, which were on the similar level as in the case when GLONASS observations were added. They also resulted in higher consistency of gradients value (w.r.t. to GPS) than adding GLONASS observations. Highest quality (in terms of standard deviation) is exhibited by a multi GNSS solution. New antenna calibration affect positively the determination of ZTD as well as tropospheric gradients (Baldysz et al., 2017).

The impact of GNSS processing strategies on the long-term parameters of 20 Years IWV time series was assessed (Baldysz et al., 2018).

Atmospheric opacity ( $\tau_0$ ) was estimated for VLBI applications basing on integrated water vapour (IWV) derived from GNSS observations in the framework of cooperation of GUT with the

Centre for Astronomy, Faculty of Physics, Astronomy and Informatics of Nicolaus Copernicus University (Nykiel et al., 2018). Two GNSS processing strategies were used (PPP and DD) with two mapping functions (VMF and GMF) to estimate ZWD which was converted in the next step to IWV. The calculated IWV was compared to  $\tau_0$  derived from the sky-dip method performed by the 32 m radio telescope located in Piwnice/Torun (Poland). The correlation between IWV and  $\tau_0$  was determined (Fig. 16) and linear regression coefficients between them were derived.

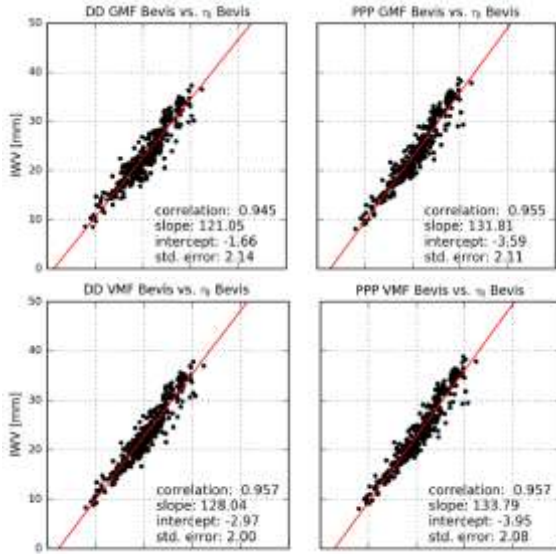


Fig. 16. Correlation between IWV and  $\tau_0$  derived from GNSS data

The results obtained indicate that IWV derived from GNSS observations may be used for calibrating archived observations from radio telescopes or for verification of obtained  $\tau_0$  values. Moreover, when the IWV is estimated in real-time mode, it can be used as a primary source of calibration data, instead of the microwave radiometer or the sky-dip method for the atmospheric opacity measurements. Both PPP and DD processing strategy can be applied for above applications.

The research group at the University of Warmia and Mazury in Olsztyn has carried out studies on optimal GNSS data processing and post-processing methodology for the estimation of tropospheric parameters. First, the study aimed at understanding the main factors leading to outliers in GPS ZTD time series in regional networks, e.g. a permanent national GNSS network. It was shown that the baseline design strategy in a double-difference network processing has a strong impact on the quality and continuity of ZTD time series. Therefore, an alternative baseline strategy that minimizes network disconnections and yields more stable ZTD time series with less outliers and gaps was developed (Stepniak et al., 2018). It was proved that using the new developed baseline design strategy the reprocessed ZTD time series are much more continuous and homogeneous in comparison to the standard strategies (Table 2).

Table 2. Statistics of ZTD estimates and formal errors (sigma) computed over 104 common ASG-EUPOS stations for three processing variants

| Strategy  | Times Max Std(ZTD) | Times Max Std(sigma) | Rejected data | Data used     | Mean Std(ZTD) [m] | Mean Std(sigma) [m] |
|---|--------------------|----------------------|---------------|---------------|-------------------|---------------------|
| "light screening": range check on ZTD [0.5 m; 3.0m], on sigma [0 m; 0.1m] |                    |                      |               |               |                   |                     |
| Standard  | 62                 | 81                   | 148           | 468332        | 0.0142            | 0.00119             |
| Obs-Max   | 31                 | 17                   | 109           | <b>471666</b> | 0.0133            | <b>0.00067</b>      |
| <b>New</b>  | <b>11</b>          | <b>6</b>             | <b>84</b>     | 469534        | <b>0.0129</b>     | 0.00079             |

In Table 1 the best values are indicated in bold. Column 2 (resp. 3) gives the number of stations for which the standard deviation of ZTD (resp. sigma) is maximum among the three solutions (e.g. standard deviation of ZTD of the old solution is maximum 62 times out of 104).

The only spikes remaining in the ZTD series in the new-developed solution are due to small number of observations or short gaps at sub-regional stations. They are removed in a post-processing screening procedure which consists in (1) the removal of the first and the last ZTD estimates around observation gaps, and (2) range check and

outlier check on ZTD and formal errors. The range check and outlier check detect spikes in ZTD and formal errors based on constant and station-specific thresholds, respectively. The screening removed about 1.2% of ZTD estimates, which remains at an acceptable level when high data continuity is required. Finally, screened GPS ZTD estimates were compared to ERA-Interim reanalysis to assess the quality of final ZTD data. The results showed good agreement between the estimates from two sources. Validation against data from climate reanalysis confirmed that GPS approach provided high-quality tropospheric delays.

The relative and precise point positioning (PPP) techniques were compared to determine more suitable one for achieving high accuracy, stability, and homogeneity in the estimated tropospheric parameters (Gołaszewski et al., 2017). Relative processing mode uses double-difference (DD) observations from a network of stations while PPP uses zero-difference observations from single stations. Relative processing is usually thought as being more precise, but not necessarily more accurate and more stable. Indeed, the estimated tropospheric parameters (ZTD and gradients) are correlated and may include biases in their absolute values when too short baselines are used. Moreover, as was proved earlier by the UWM group, the network configuration (extension and geometry of the baselines) can have a significant impact on tropospheric parameters in double-difference processing. PPP is an absolute technique in the sense of no propagation of errors between stations. However, the accuracy of data processing in PPP mode depends strongly on the quality of external products, like satellite orbits and clocks. Data processing in PPP mode is also faster than DD solution, because only observations for the stations of interest are processed while in relative processing additional stations are required to form long baselines and reduce the correlation between tropospheric parameters. It was assumed that PPP might be an interesting alternative to double-difference processing for estimation of tropospheric parameters, especially in cases when outliers arising from defects in the baseline geometry in a double-difference processing (Fig. 17).

In GNSS data processing the station height, receiver clock and tropospheric delay (ZTD) are highly correlated to each other. Although the zenith hydrostatic delay (ZHD) of the troposphere can be provided with sufficient accuracy, zenith wet delay (ZWD) has to be estimated, which is usually done in a random walk process. Since ZWD temporal variation depends on the water vapour content in the atmosphere, it seems to be reasonable that ZWD constraints in GNSS processing should be geographically and/or time dependent. Taking benefit from numerical weather prediction models to define optimum random walk process noise was proposed at WUELS. In the first approach archived VMF1-G data were used to calculate a grid of yearly (Fig. 18) and monthly means of the difference of ZWD between two consecutive epochs divided by the root square of the time lapsed, which can be considered as a random walk process noise.

Alternatively, the Global Forecast System (GFS) model from National Centres for Environmental Prediction (NCEP) was used to calculate random walk process noise dynamically in real-time. Hadas et al. (2017b) performed two representative

experimental campaigns with 20 globally distributed IGS stations and compared real-time ZTD estimates with the official ZTD product from the IGS. Both approaches exhibit an improvement of up to 10% in accuracy of the ZTD estimates compared to any uniformly fixed random walk process noise applied for all stations.

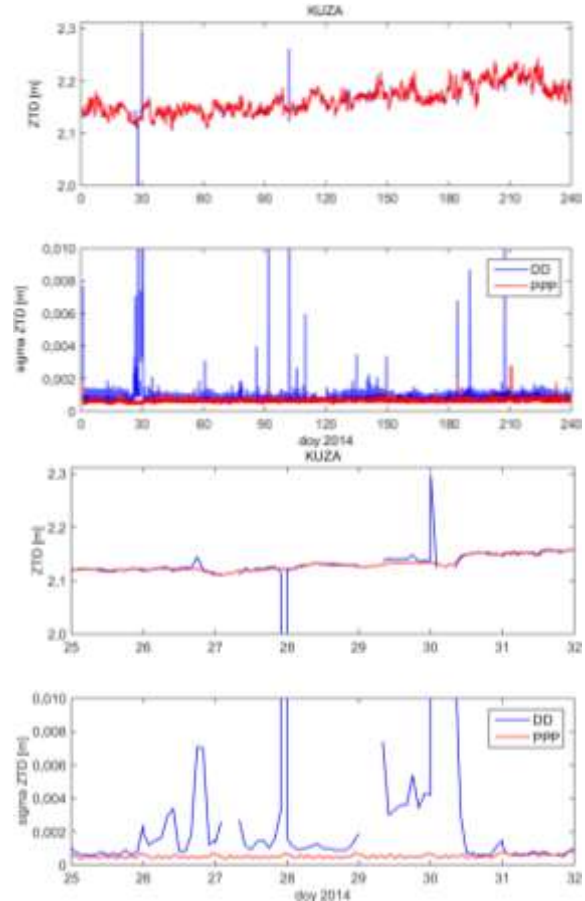


Fig. 17. Comparison of ZTD estimates and formal error for the DD and PPP solutions (upper two graphs); zoom on period when the DD solution has outliers due the geometry of the network (lower two graphs)

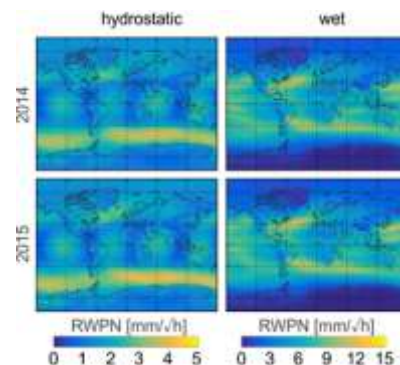


Fig. 18. Hydrostatic (left) and wet (right) yearly mean RWPN grids over 2012-2015

Real-time GNSS troposphere estimation operational system for zenith troposphere delay estimation was established using a modified version

of PPP-WIZARD software. In the computation three navigational satellite systems: GPS, GLONASS and Galileo were used. Real-time observations supported by the real-time clocks and orbit corrections were employed. The obtained real-time ZTD is assessed on the basis of the initialization time and the obtained accuracy (Fig. 19). The IGS/MGEX real-time streams and the real-time products applied were provided by Le site du Centre national d'études spatiales (CNES).

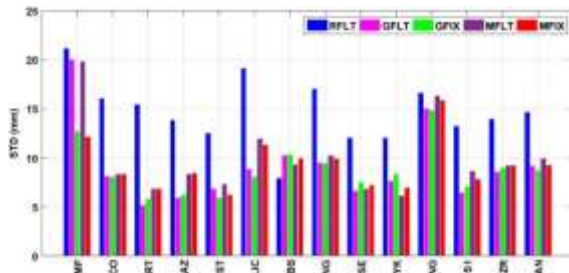


Fig. 19. STD of RT ZTD errors with respect to the radiosonde observations in all data processing modes

Considering the convergence time the results reveal different time for GLONASS-only and GPS-only solution. The required time when using GLONASS-only equals to 1364 s and 613 s when using GPS-only. This time can be shortened by applying real-time PPP ambiguity resolution and by using GPS, GLONASS and Galileo observations. Initialization process can be finished in an average time of 508 s when using three constellations and when PPP ambiguity resolution is applied.

To determine the accuracy, the obtained results were compared to the final troposphere products from CODE and USNO, as well as to the radiosonde observations. The conducted comparisons show that the real-time troposphere generated with a single system or multi-system observations is accurate enough to fulfil the accuracy requirements for nowcasting. Real-time PPP ambiguity can improve the accuracy more than a combination of multisystems observations in opposition to the initialization time case (Ding et al., 2017).

Improvement of the EGNOS GNSS augmentation (Kazmierski et al., 2017) was investigated in WUELS. The EGNOS/UNB3m model was adjusted to the actual measured meteorological parameters which could be applied into EGNOS. The model is called UNBe.eu, wherein the letter e stands for EGNOS and letters eu for the European area. The reasoning behind this study is based on the fact that ZTD estimates are incorrect for some locations. The study area ranges from 20 to 70° in latitude and from -40 to +40° in longitude.

The process described in this article allowed for creating a model using values of meteorological

parameters measured directly at the stations in Europe. The obtained results from the new and classical models were compared to ZTD obtained from radio sounding observations. The newly established model provides comparable or more accurate results than the UNB3m model in terms of both the bias and RMS for the majority of the tested stations (for more than 70% of them). The meteorological observations were available for most stations and their ZTD estimation outcomes are deemed satisfactory (Fig. 20). Unfortunately, there were also a few examples of locations, especially near oceans and seas, for which the results obtained by UNBe.eu were less accurate than those obtained by UNB3m. Those water masses may have affected the measurements. Consequently, it may have led to the annual variation of ZTD parameters that occurred to be underestimated, leading to problematic or incorrect estimates of ZTD amplitudes.

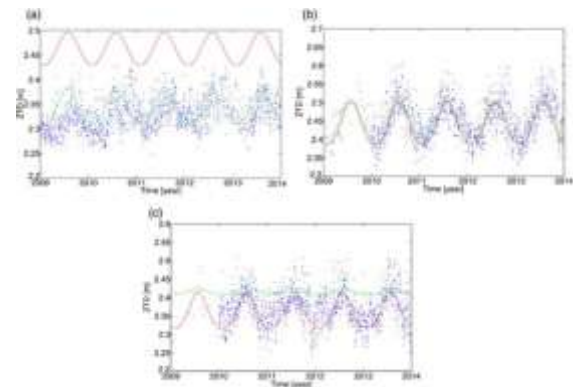


Fig. 20. ZTD estimation results for UNBe.eu (green) and UNB3m (red) model: a ID 62414, Lat = 23.9700, Lon = 32.7800, H = 194.0 m, b ID 7761, Lat = 41.9200, Lon = 8.8000, H = 5.0 m, c ID 3005, Lat = 60.1300, Lon = -1.1800, H = 82.0 m, blue dots – ZTD calculated

WUELS team took part in the framework of EU COST ES1206 Action in the research on the estimation of slant troposphere delays of GNSS signal (Kačmařík et al., 2017). An extensive validation of line-of-sight tropospheric slant total delays (STD) from GNSS, ray tracing in numerical weather prediction model (NWM) fields and microwave water vapour radiometer (WVR) was presented. Inter-techniques evaluations demonstrated a good mutual agreement of various GNSS STD solutions compared to NWM and WVR STDs. The mean bias among GNSS solutions not considering post-fit residuals in STDs was -0.6 mm for STDs scaled in the zenith direction and the mean standard deviation was 3.7 mm. Standard deviations of differences between GNSS and NWM ray-tracing solutions were typically 10 mm ± 2 mm (scaled in the zenith direction), depending on the NWM model and the GNSS station. Comparing GNSS versus WVR STDs reached standard

deviations of  $12\text{ mm} \pm 2\text{ mm}$  also scaled in the zenith direction. Impacts of raw GNSS post-fit residuals and cleaned residuals on optimal reconstructing of GNSS STDs were evaluated at inter-technique comparison and for GNSS at collocated sites. The use of raw post-fit residuals is not generally recommended as they might contain strong systematic effects, as demonstrated in the case of station LDB0. Simplified STDs reconstructed only from estimated GNSS tropospheric parameters, i.e. without applying post-fit residuals, performed the best in all the comparisons; however, it obviously missed part of tropospheric signals due to non-linear temporal and spatial variations in the troposphere. Although the post-fit residuals cleaned of visible systematic errors generally showed a slightly worse performance, they contained significant tropospheric signal on top of the simplified model. They are thus recommended for the reconstruction of STDs, particularly during high variability in the troposphere. Cleaned residuals also showed a stable performance during ordinary days while containing promising information about the troposphere at low-elevation angles.

### Monitoring ionosphere and ionospheric storms

Research concerning the development of the efficient approach to mitigate the impact of the most frequent ionospheric wave signatures: the medium-scale traveling ionospheric disturbances (MSTIDs) in precise GNSS positioning was conducted at the Institute of Geodesy of the University of Warmia and Mazury in Olsztyn (IG/UWM) and in WUELS in cooperation with the team from Spain. The direct GNSS Ionospheric Interferometry technique impact on precise positioning is that one can obtain reliable RTK position faster – reduction of the time-to-fix (Hernández-Pajares et al., 2017). The performance of the technique is demonstrated with networks of GNSS receivers in Poland, treated as users under real-time conditions, during two representative days in winter and summer seasons (days 353 and 168 of year 2013). Researchers from WUELS investigated a potential improvement in troposphere estimation, and tested two different strategies of baseline configuration, namely SHORTEST and STAR (Fig. 21). However, due to any potential impact of the MSTID mitigation model, the differences in troposphere domain were most difficult to demonstrate.

The team of GUT in collaboration with the team of the Department of Radiophysics of Geospace of the Institute of Radio Astronomy NAS of Ukraine in Kharkiv develop the original solution for the estimation of ionospheric total electron content (TEC) variations using satellites with elevation angles over  $70^\circ$  (Nykiel et al., 2017). The use of

high elevation angle satellites allows to obtain the ionospheric variation model immediately over the selected area and without large errors associated with an incorrectly taken layer height. However, here is no possibility to use this advantage at high latitudes. A high spatial resolution of the IPPs can be obtained by using the dense regional networks of GNSS stations, such as ASG-EUPOS, SAPOS, etc. Representative examples of TEC variation spatial distribution are presented in Figure 22.

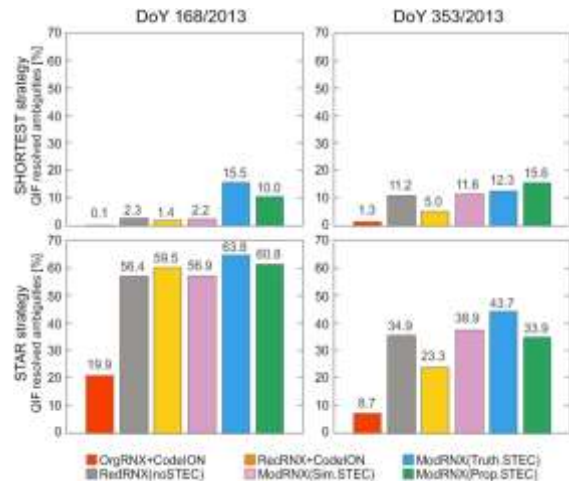


Fig. 21. Percent of QIF resolved ambiguities in (top row) SHORTEST and (bottom row) STAR baseline definition strategies, during (left column) summer and (right column) winter campaigns, for six different network solutions

The possibility of developing maps of TEC variations with the resolution of tens of kilometres, with the temporal rate of tens of seconds was demonstrated. Such maps allow to analyse the structure and temporal evolution of mesoscale ionospheric irregularities. In accordance with current trends in the development of a four-dimensional (4D) geodesy, the use of the proposed methodology makes it possible to obtain and effectively use a large amount of information organized in the form of time sequences of maps.

Investigation of some magnetospheric phenomena of geomagnetic storm on March 17, 2013 based on observations from GNSS and NOAA-15 satellite was conducted (Zanimonskiy et al., 2017).

## 5. Advanced methods for satellite positioning

The research group at the University of Warmia and Mazury (UWM) in Olsztyn has carried out extensive studies concerning theoretical analysis and practical assessment of the selected models for multi-constellation signals integration (Paziewski and Wielgosz, 2017). The assessment of the analyzed strategies was based on the performance analyses of the integer ambiguity resolution and rover coordinates' repeatability obtained in the

medium range instantaneous RTK positioning with full constellation GPS and Galileo signals. Since at that time the full constellation of Galileo satellites was not yet available, the observational data were obtained from hardware GNSS signal simulator and regular geodetic GNSS receivers. The results indicated similar and high-performance of the

loosely, and tightly integrated model with calibrated receiver ISBs strategies. The approaches proved undeniable advantage over single system positioning in terms of reliability of the integer ambiguity resolution as well as rover coordinate repeatability.

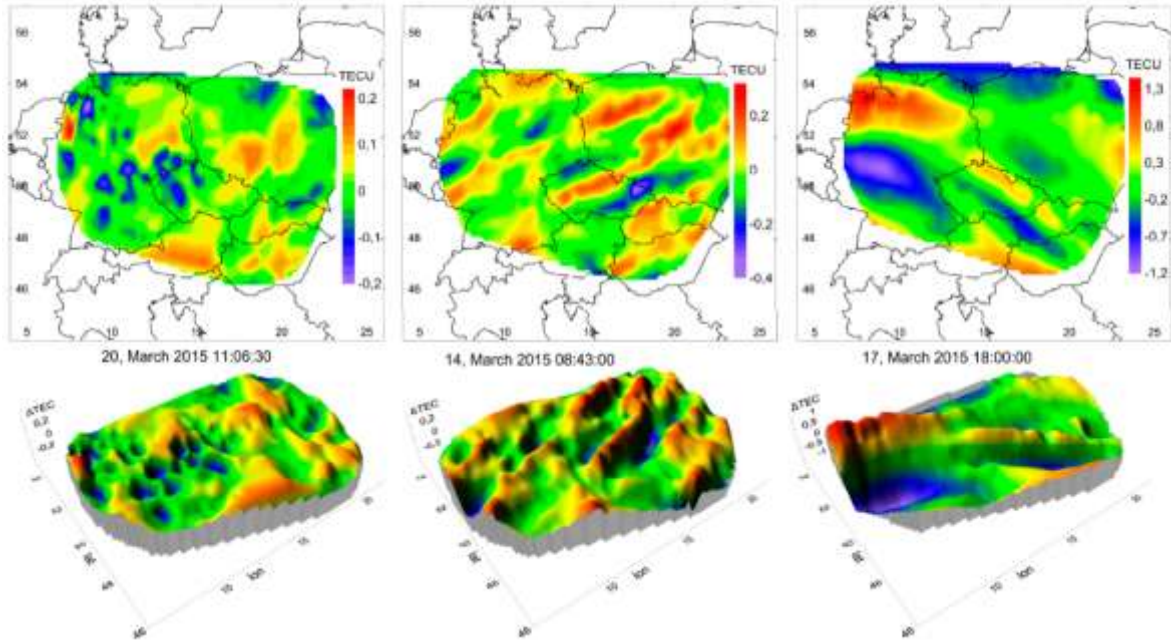


Fig. 22. Representative examples of spatial distribution of TEC variation

Theoretical foundations and performance assessment of instantaneous medium-range GPS+BDS RTK based on real signals collected at the territory of China were described (Paziewski and Sieradzki, 2017). These studies were preceded by the analysis of measurement noise for both aforementioned systems. The considerable differences of code observation noise, which should be taken into account in stochastic modelling, were confirmed. The study of dispersion of code pseudorange observations caused by combined multipath and noise effect has confirmed slightly higher precision of code signals on the first in respect to second frequency for both GPS and BDS constellations. The more comprehensive analysis suggested that in the case of strong ionospheric disturbances, the internal smoothing of code observations can be a source of their strong discrepancies. Due to the length of baselines (several dozens of km) the investigation of phase measurement noise was based on triple differenced observations. Generally, the results have revealed the similar level of phase noise for both systems. Only for geostationary BDS satellites one can observe measurable higher values. The study

proved also benefits from multi-constellation signals to the reliability, accuracy and time-to-fix in GPS + BDS RTK positioning. This was investigated on the basis of experiment simulating different observing conditions – with terrain obstacles. The advantage of multi-GNSS positioning in harsh observing conditions was proved. The application of data from both GNSS systems allowed instantaneous position solution even with high elevation mask.

The tropospheric delay is one of the major error sources in Precise Point Positioning (PPP), affecting the accuracy and precision of estimated coordinates and convergence time, which raises a demand for a reliable tropospheric model, suitable to support PPP. The impact of three different tropospheric models and mapping functions on the position accuracy and convergence time was investigated at Wrocław University of Environmental and Life Sciences (WUELS). The routine to constrain the tropospheric estimates (Wilgan et al., 2017) was implemented in the in-house developed real-time PPP software. The advantage of the high spatial resolution (4 km × 4 km) Numerical Weather Prediction (NWP) Weather Research and Forecasting (WRF) model was taken to reconstruct

troposphere delay from the WRF and near real-time GNSS data combined by the least-squares collocation technique. Mapping functions calculated from WRF model using the ray-tracing technique are also presented. The performance tests are conducted on 14 Polish EUREF Permanent Network (EPN) stations during three weeks of different tropospheric conditions: calm, standard and severe. Six GNSS data processing variants were considered, including two commonly applied variants using a priori ZTD and mapping functions from UNB3m and VMF1-FC models, one with a priori ZTD and mapping functions calculated directly from WRF model and three variants using the aforementioned mapping functions but with ZTD model based on GNSS and WRF data used as a priori troposphere and to constrain troposphere estimates. The application of a high-resolution GNSS/WRF-based ZTD model and mapping functions results in the best agreement with the official EPN coordinates. In both static and kinematic mode, this approach results in average reduction of 3D bias by 20 and 10 mm, respectively, but an increase of 3D standard deviations by 1.5 and 4 mm, respectively (Fig. 23). The application of high-resolution tropospheric model also shortens the convergence time, e.g. for 10 cm convergence level from 67 min to 58 min for the horizontal components and from 79 min to 63 min for the vertical component.

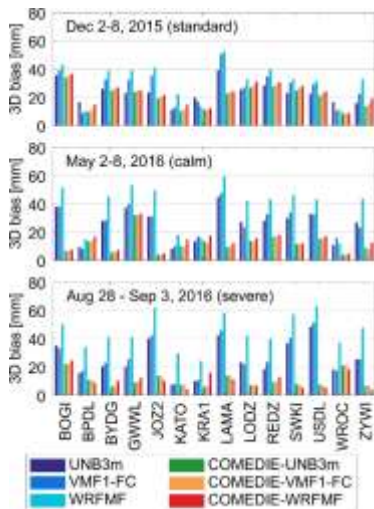


Fig. 23. Mean 3D biases of kinematic coordinate residuals for 14 Polish EPN stations for three data periods and all kinds of troposphere augmentation methods

The cooperation of WUELS with the Ohio State University (USA) resulted in research on positioning of slow-moving platforms by UWB technology in GPS-challenged areas. Ultra-wideband (UWB) radio networks are low-power, simple, and easily deployable local systems that may be used for navigation and positioning

purposes. The properties of the UWB signal are attractive because they can go through obstacles, providing potential positioning in environments where other systems are not suitable, such as interior of buildings or dense forest. UWB-network positioning was used to support accurate geolocalization of slow-moving vehicles in environments that challenge global navigation satellite systems (GNSSs), such as forested areas. Toth et al. (2017) analyze the results of several experiments with land vehicle positioning (Fig. 24) within a UWB network in various outdoor and indoor scenarios. The influence of obstacles on signal propagation and, ultimately, on range measurements and the motion compensation resulting from the low UWB-data acquisition rates are discussed in detail. Results show that the tested equipment within an area of approximately  $30 \times 30$  m can achieve positioning accuracy of 10 to 30 cm, depending on the environmental parameters and UWB-network configuration.



Fig. 24. Slow-moving vehicle and measurement setup

Following studies devoted to the higher-order ionospheric effects proved that modelling of these terms affects the estimated coordinates at the level of a few millimeters in PPP and at negligible level considering medium-range RTK. As shown in (Banville et al., 2017), the parametrization of higher-order effects in the PPP solution lead to the propagation of DCB into the receiver position.

High precision Global Navigation Satellite Systems (GNSS) positioning and time transfer require correcting signal delays, in particular higher-order ionospheric ( $I_2^+$ ) terms. A consolidated model to correct second- and third-order terms, geometric bending and differential STEC bending effects in GNSS data was presented (Hadas et al., 2017a). The model has been implemented in an online service correcting observations from submitted RINEX files for  $I_2^+$  effects. GNSS data processing was performed with and without including  $I_2^+$  corrections, in order to investigate the impact of  $I_2^+$  corrections on GNSS

products. WUELS used GPS and GLONASS observations from a global network and two regional networks in Poland and Brazil for three time periods representing different ionospheric conditions. Satellite orbits, satellite clock corrections, Earth rotation parameters, troposphere delays, horizontal gradients, and receiver positions were estimated using a global GNSS solution and PPP techniques. The satellite-related products captured most of the impact of I2+ corrections, with the magnitude up to 2 cm for clock corrections, 1 cm for the along- and cross-track orbit components, and below 5 mm for the radial component. The impact of I2+ on troposphere products turned out to be insignificant in general. I2+ corrections caused a systematic shift in the coordinate domain that was time- and region-dependent, and reached up to -11 mm for the North component of the Brazilian stations during the most active ionospheric conditions (Fig. 25).

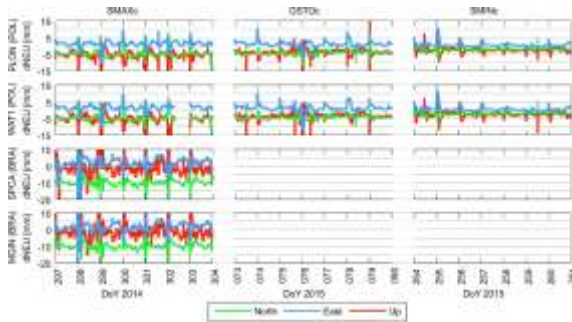


Fig. 25. Time series of kinematic coordinate differences between the solutions without and with I2+ corrections for selected test sites: PLON, WAT1 (in Poland), SPCA and MGIN (in Brazil) over 3 test periods

The original processing algorithms developed allowed for practical application of the GNSS technology to determination ground deformations as well as dynamic displacements including these of engineering structures (Malyszko et al., 2017; Paziewski et al., 2017; Stępnik et al., 2017).

The research group from GUT investigated the impact of Galileo observations on multi-GNSS positioning and products. Positioning results obtained with five different combinations of GNSS systems: GPS, Galileo, GPS/Galileo, GPS/GLONASS and GPS/GLONASS/Galileo were presented focusing on the precision of the position determination (Nykiel and Figurski, 2017). The results obtained using Galileo only observations exhibit the highest standard deviations which is due to the low number of the Galileo satellites. However, even when the constellation is not complete, the differential precise positioning using only Galileo observations can provide the horizontal and vertical precision below 1 cm (Fig. 26).

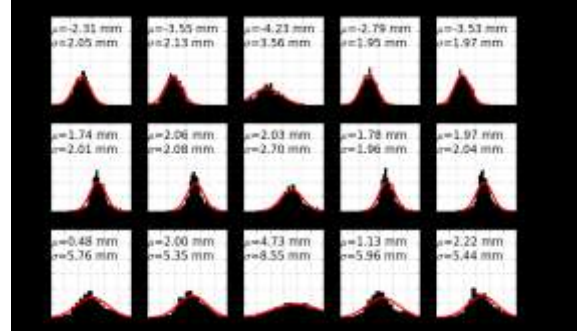


Fig. 26. Histograms of the residuals for all analyzed solutions after week 1920; from the top: North, East and Up coordinates

The Galileo observations have significant impact on the multi-GNSS positioning results. Highest precision (1.95 mm) in the horizontal coordinates and the lowest bias all coordinates were obtained using the combination of GPS and Galileo data. Better precision in Up coordinate was obtained from GPS/GLONASS solution, i.e. 5.35 mm as compared with 5.96 mm from GPS/Galileo.

The resolution for ambiguities for wide-lane (WL) and narrow-lane (NL) linear combination (Fig. 27) was also analysed.

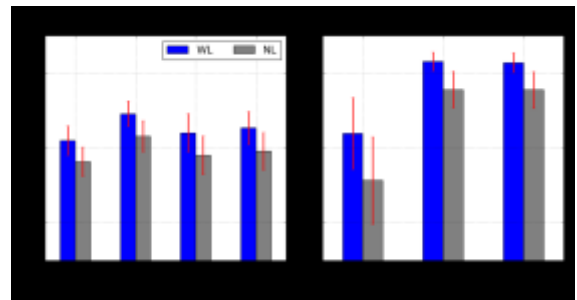


Fig. 27. Mean percentage of GPS and Galileo WL (blue) and NL (grey) ambiguity resolutions for tested solutions

After the EOC and the few weeks before that date, the mean ambiguity resolution for the Galileo satellites amounted to  $80.85 \pm 4.31\%$  and  $70.97 \pm 5.68\%$ , for WL and NL, respectively. In the case of multi-GNSS positioning, the best results of ambiguity resolution for GPS and Galileo satellites were obtained for GPS\_GAL solution; the mean value of the WL ambiguity resolutions was  $79.15 \pm 3.45\%$  for GPS and  $93.14 \pm 2.45\%$  for Galileo. In the case of both position determination and ambiguity resolution, the best results exhibited GPS/Galileo solution (even better than GPS/GLONASS/Galileo solution), not the GPS/GLONASS solution used and recommended by the EUREF. With the increasing number of Galileo satellites the precision of positioning should be even better, especially in the Up coordinate. It seems that position determination using GPS/Galileo will be more efficient than GPS/GLONASS or even GPS/GLONASS/Galileo,

especially, when considering computation time of multi-GNSS observations.

Differences of antenna Phase Center Corrections (PCC) between antenna individual calibration for Galileo E5 frequency and for GPS L2 frequency estimated within the range from -6 to 8 mm indicate that copying calibration from L2 to E5, as it was often done before, can cause significant errors. The computation tests performed proved that the use of antenna models for Galileo frequencies makes sense only when all station in the network support such calibration. In Figure 28 two solutions for BRUX station: GAL\_14, marked with red line, where individual calibrations were used; and GAL, grey line, where calibration for Galileo E5 were copied from GPS L2 are presented. Based on the presented results a bias between solutions reaching 8.5 cm is observed in Up coordinate. It is worth to note that the use of individual calibration caused only bias change without changing standard deviations (Nykiel and Figurski, 2017).

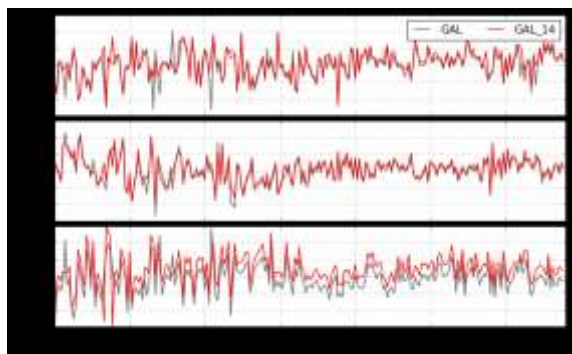


Fig. 28. Galileo only positioning results for BRUX station for two solutions: with IGS14 antenna model - GAL\_14 (red line); GAL (grey line)

The impact of DMI measurements on a position estimation with lack of GNSS signals during Mobile Mapping was investigated at GUT (Bobkowska et al., 2017).

## 6. ASG-EUPOS network

### 5.1. Status of the ASG-EUPOS network

At the end of 2017 the network of the ASG-EUPOS system consisted of 125 operating permanent reference stations (all of them track GPS and GLONASS; 107 track also Galileo satellites, of which 86 track in addition BDS satellites) (Fig. 29) ([www.asgeupos.pl](http://www.asgeupos.pl)).

At the end of 2017 12 GNSS receivers and antennas were purchased to replace the remaining sets with only GPS and GLONASS tracking capabilities. Exchange of the equipment is planned for II quarter of 2018 after individual antennae calibration.



Fig. 29. Reference stations of the ASG-EUPOS system (31 December 2017)

Since 12 July 2014 when all services in ASG-EUPOS system became fully payable, the total number of users with activated subscriptions reached 6510. At the end of 2017 the number of active users for RTN, RTK and DGNS services reached 3613 where the average number of users accessing the system every working day exceeds 2100.

Further modernization of the ASG-EUPOS system is planned in 2018. A software in the system management centres will be updated. RTN correction data from GPS, GLONASS, Galileo and BDS will be provided for the whole area of Poland.

Spatial pattern of ASG-EUPOS sites was investigated (Calka et al., 2017).

## 7. Modelling precise geoid

Activities of the team of the Institute of Geodesy and Cartography (IGiK) on the improvement of the accuracy of precise quasigeoid modelling for Poland were continued. The use of scattered/sparse absolute gravity data for the validation of Global Geopotential Models and for improving quasigeoid heights determined from satellite-only Global Geopotential Models was extensively investigated (Godah et al., 2018).

The gravity anomalies obtained from GGMs were validated with absolute gravity determined with the A10-020 gravimeter at 161 gravity stations of the modernized Polish gravity control network using the spectral enhancement method. The quasigeoid heights obtained from the satellite-only GGM as well as from the satellite-only GGM in combination with absolute gravity data were evaluated with high accuracy GNSS/levelling data. It was shown that adding absolute gravity data to the satellite-only GGM results in an improvement of quasigeoid model developed by a factor of 2.5. The spatial resolution and the accuracy of the quasigeoid model obtained from satellite-only

GGMs can be improved from approx. 100 km to 40 km and from ca. 24 cm to ca. 10 cm, respectively. The results obtained, demonstrate the capability of absolute gravity data measured by the A10 absolute gravimeter for the validation of GGMs as well as for improving geoid/quasigeoid heights obtained from satellite-only GGMs. Thus, the establishment of a gravity network using an absolute gravimeter, especially for areas with a lack of high quality satellite/levelling data and insufficient coverage with terrestrial gravity data, is strongly recommended.

Current state of art of satellite altimetry was discussed at the Koszalin University of Technology (Lyszkowicz and Bernatowicz, 2017). Special attention was paid on the use of altimetry for monitoring elevations of continental surface water. A case study in Poland concerning variation of the surface elevation of the Lebsko lake in was conducted. The results obtained reveal that altimetry could be a promising tool for true global lake studies with accuracy at centimetre level (Bernatowicz and Lyszkowicz, 2017).

Currently available gravity anomalies from satellite altimetry models were validated along the Polish coast and in the Baltic Sea with the use of shipborne and airborne gravity anomalies at the University of Warmia and Mazury in Olsztyn. New gravity data from the satellite altimetry, the EIGEN-6C4 geopotential model, and the SRTM model were then used for developing the new gravimetric quasigeoid model for the territory of Poland. Its accuracy estimated using the ASG-EUPOS permanent GNSS stations reaches 1.4 cm (Kuczynska-Siehien and Lyszkowicz A, 2017).

## 8. The use of data from satellite gravity missions

Quality of the newest satellite only 5 global geopotential models IGGT\_R1, IfE\_GOCE05s, GO\_CONS\_GCF\_2\_SPW\_R5, Tongji-Grace02s, and NULP-02s as well as XGM2016 model combined with terrestrial data was investigated in IGIK. They were evaluated in terms of height anomalies using GNSS/levelling data at ASG-EUPOS stations. The fit of models up to d/o 200 (except Tongji-Grace02s developed to d/o 180) to satellite/levelling data was at the level of 24 cm. Such fit using maximum d/o of the models is shown in Table 3. Obtained results indicate poor quality of spherical harmonics above d/o 200 in satellite-only models investigated.

The use of the Principal Component Analysis/Empirical Orthogonal Function (PCA/EOF) method for the analysis and modelling temporal variations of geoid heights was investigated (Godah et al., 2017a). The results revealed that ~99.93% of total variance of temporal variations of geoid heights can be obtained using the first three PCA modes and EOF loading patterns. The significant signal, i.e. greater than 96.3% in terms of total variance, of temporal variations of geoid heights over the area of Poland can be obtained from the first PCA mode and EOF loading pattern. Models of temporal variations of geoid heights developed using the PCA/EOF method are satisfactory. The fit, in terms of the standard deviations of the differences between temporal variations of geoid heights models obtained with the use of the PCA/EOF method, and the respective ones determined from RL05 GRACE-based GGMs is of 0.3–0.4 mm.

Table 3. Statistics of the differences between geoid heights obtained from GGMs and the corresponding satellite/levelling ones for the ASG-EUPOS stations [m]

| GGM                  | Maximum d/o | Min    | Max   | Mean  | Std   |
|----------------------|-------------|--------|-------|-------|-------|
| IfE_GOCE05s          | 250         | -0.530 | 0.546 | 0.025 | 0.223 |
| IGGT_R1              | 240         | -0.380 | 0.533 | 0.054 | 0.195 |
| NULP-02s             | 250         | -0.493 | 0.530 | 0.040 | 0.232 |
| GO_CONS_GCF_2_SPW_R5 | 330         | -0.459 | 0.535 | 0.028 | 0.210 |
| Tongji-Grace02s      | 180         | -1.005 | 0.882 | 0.058 | 0.364 |
| XGM2016              | 719         | -0.138 | 0.144 | 0.077 | 0.041 |

Temporal variations of geoid heights obtained from RL05 GRACE-based GGMs were investigated

over the Central Europe represented by 16 subareas (Fig. 30) (Godah et al., 2017b) as well as over the

area of Poland represented by 4 subareas (Fig. 31) (Godah et al., 2017c).

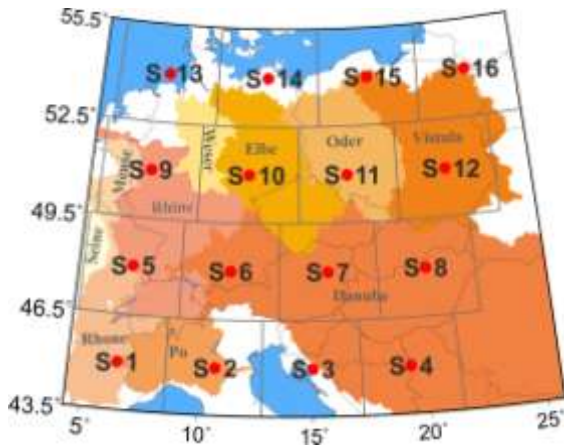


Fig. 30. Subareas of Central Europe for which geoid height variations were investigated with major river basins

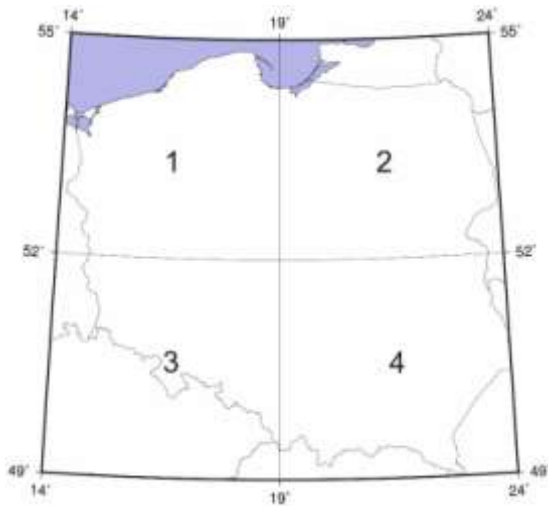


Fig. 31. Subareas in Poland for which geoid height variations were investigated

Physical height changes over Central Europe for the period between January 2004 and December 2010 reach up to 22.8 mm. The obtained physical height changes can be modelled with an accuracy of 1.4 mm using the seasonal decomposition method (Godah et al., 2017b).

In the absolute sense, i.e. at the same  $3^\circ \times 5^\circ$  subarea of Poland, geoid height variations differences from epoch to epoch can reach 10 mm. In the relative sense, i.e. from one  $3^\circ \times 5^\circ$  subarea to another, temporal geoid height variations differences between two subareas can reach 2 mm at the same epoch and 11 mm at different epochs (Godah et al., 2017c).

Groundwater level variations and water balance in the area of the Sudety Mountains were analysed by the team of the University of Warmia and Mazury for the period of November 2002 - October 2015 (Rzepecka et al., 2017) using the mean Terrestrial Water Storage (TWS) obtained from

GRACE data and data from Global Land Data Assimilation System (GLDAS). The groundwater level declined by about 13 cm (approximately 1 cm/year) over the period investigated.

The ARIMA (or ARMA) models, together with exponential smoothing and structural models, methods were tested for forecasting future behaviour of time series to find most suitable method for the computation of the water budget and accuracy assessment of the ground water level determination (Birylo et al., 2017). It was shown that the greatest influence on the final water budget value have snow and rain falls (precipitation). A comparison between the real water budget data and the prediction for twelve months in the period of 2015.08 – 2016.08 proved that the use of ARIMA models provides best forecast results.

Seasonal variability of the atmospheric (energy) and water budgets in Poland were investigated in terms of total water storage using the GLDAS data. The Modern-Era Retrospective analysis for Research and Applications version 2 (MERRA-2), and GRACE data (Birylo, 2017a, 2017b). Results from GLDAS and MERRA-2 models showed good agreement. No linear correlation between the total water storage and the atmospheric budget was observed.

A geophysical interpretation of polar motion based on the GRACE data and hydrological models was investigated by the team of the Space Research Centre of the Polish Academy of Sciences. Hydrological polar motion excitation functions were re-estimated using the most recent geopotential models developed in seven processing centres on the basis of GRACE data. The results obtained were compared with the respective ones determined from two hydrological models GLDAS and LSDM as well as two climate models CMIP5 – Miroc5 and MPI-ESM-LR (Winska et al., 2017).

The agreement between geodetic residuals (GAO) and different determinations of hydrological excitation functions (HAM) computed both from GRACE data and hydrological and climatic models was examined. Global time series of non-seasonal  $\chi_1$  and  $\chi_2$  components (for short-term oscillations, i.e. with periods under 730 days and long-term oscillations, i.e. with periods over 730 days) of mean geodetic residuals (Mean GAO), gravimetric excitation functions from GRACE (CSR, JPL, GFZ, HUST, TONGJI, WHU, CNES) and hydrological excitation functions from various models (GLDAS, LSDM, MIROC, MPI) are presented in Figure 32.

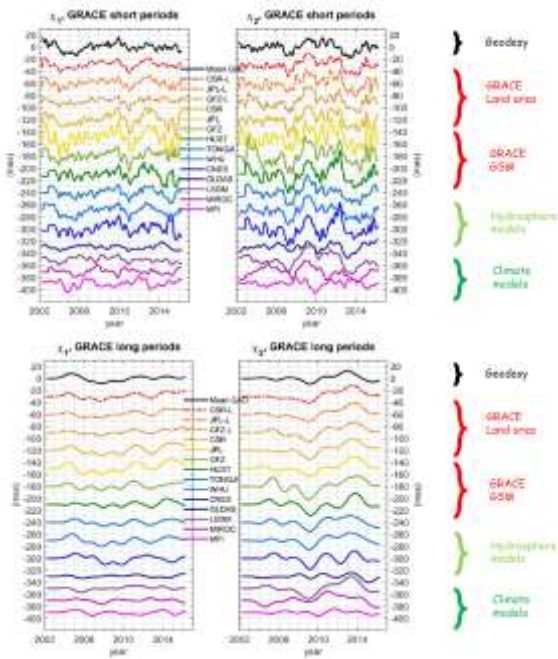


Fig. 32. Short period (a), and long period (b) variations of  $\chi_1$  and  $\chi_2$  components of mean geodetic residuals (M GAO) with gravimetric (CSR, JPL, GFZ, HUST, TONGJI, WHU, CNES) and hydrological (GLDAS, LSDM, MIROC, MPI) excitation functions; solid lines show gravimetric excitation computed from the GSM coefficient, dotted lines reflect contributions over the land area only

### 9. Monitoring gravity changes

Earth tides were continued to be monitored in 2017 at the Borowa Gora Observatory of IGiK with the LCR G-1036 gravimeter equipped with the LRFB-300 feedback system. Gravity record from 2012-2017 acquired with the LCR G-1036 gravimeter was processed using Fourier transform to determine its spectral characteristics (Fig. 33).

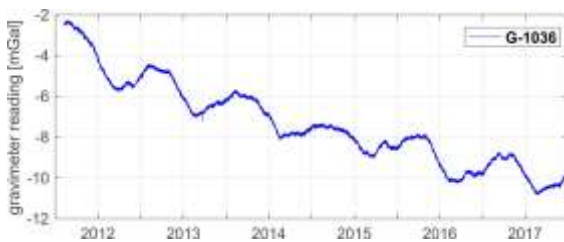


Fig. 33. Gravity record with LCR G-1036 gravimeter at Borowa Gora Observatory, averaged in 1 hour window

A continuous gravity signal was collected in 2017 by the iGrav-027 superconducting gravimeter at the Borowa Gora Geodetic-Geophysical Observatory with 1 second sampling rate. Recorded tidal variations of gravity resampled to 1 minute are shown in Figure 34.

Further analysis of tidal data was conducted using the ETERNA 3.40 software. Parameters of the new local tidal model for Borowa Gora were determined. The residua of tidal adjustment obtained from the using the ANALYZE software,

their power density spectrum and their histogram are given in Figure 35.

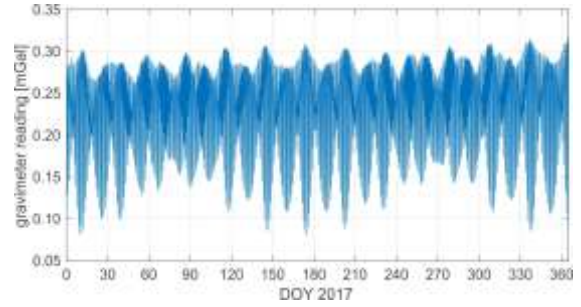


Fig. 34. Tidal record with the iGrav-027 gravimeter in 2017

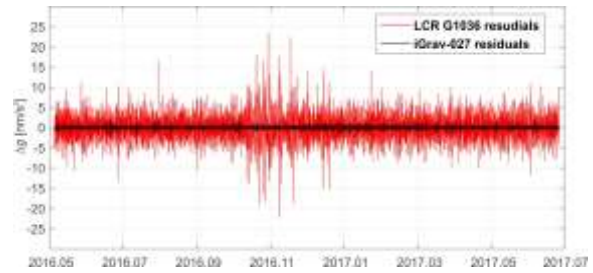


Fig. 35. Residuals from tidal adjustment with the use of high pass filter

### 10. Activity in Satellite Laser Ranging and their use

In 2017 the Satellite Laser Ranging station BORL at Borowiec of the Space Research Center of the Polish Academy of Sciences tracked 36 different objects, cooperative and uncooperative targets, in a total of 838 full passes (Fig. 36).

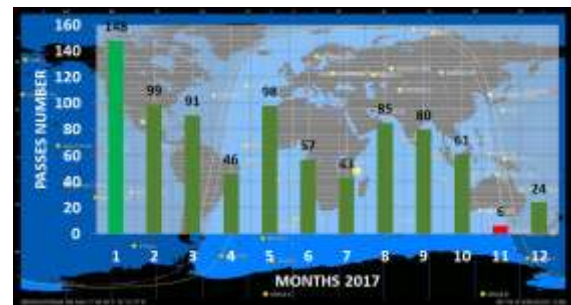


Fig. 36. Observational statistics (Satellites + Debris) for BORL station in 2017

24 of these objects (20 LEO and 4 MEO) were satellites from the ILRS list ([https://ilrs.cddis.eosdis.nasa.gov/missions/satellite\\_missions/current\\_missions/](https://ilrs.cddis.eosdis.nasa.gov/missions/satellite_missions/current_missions/)). The average RMS ranged from 1.28 cm to 6.52 cm (587 passes, 564 367 returns and 9 947 normal points). All the results were sent to the data banks at NASA's Crustal Dynamics Data Information System (CDDIS) and the Eurolas Data Center (EDC).

The other 12 objects were typical space debris, inactive (defunct) satellites and rocket bodies from

the LEO regime. Space debris targets were observed in the framework of the Space Debris Study Group (SDSG) of the ILRS (International Laser Ranging Service). A total of 251 space debris passes were performed with the average RMS ranging from 5.18 cm to 81.60 cm (251 passes, 230 901 returns and 3 529 normal points). All the results were sent to the SDSG data bank.

From all tracked satellites 7 were typical passive geodetic-geodynamic satellites (Ajisai, Lageos-1, Lageos-2, Larets, Lares, Starlette and Stella) which gave in total 265 passes, 294 934 single good shots and 3 154 normal points. All results obtained by BORL station in 2017 are available in graphical form at [http://www.cbk.poznan.pl/stacja\\_laserowa/lista\\_observacji\\_2017.php](http://www.cbk.poznan.pl/stacja_laserowa/lista_observacji_2017.php).

The quality of the BORL laser sensor is evaluated regularly based on tracking results of LAGEOS-1 and LAGEOS-2 satellites in the form of station performance report. As results from Figures 37 and 38, the BORL station significantly improved the quality and effectiveness of the measurements in comparison to the previous years of its activity.

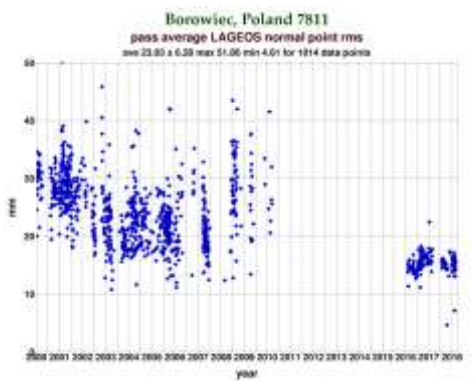


Fig. 37. LAGEOS normal point RMS since 2000 to 2018 for BORL station (source: [https://ilrs.cddis.eosdis.nasa.gov/network/stations/charts/BORL\\_LAG\\_NPT\\_RMS.png](https://ilrs.cddis.eosdis.nasa.gov/network/stations/charts/BORL_LAG_NPT_RMS.png))

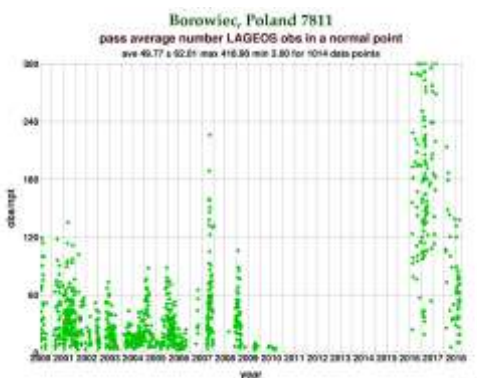


Fig. 38. LAGEOS measurements in a normal point since 2000 to 2018 for BORL station (source: [https://ilrs.cddis.eosdis.nasa.gov/network/stations/charts/BORL\\_LAGEOS\\_NPT\\_OBS.png](https://ilrs.cddis.eosdis.nasa.gov/network/stations/charts/BORL_LAGEOS_NPT_OBS.png))

The laser ranging measurements from BORL 7811 station support global research in satellite and space debris rotation (tumbling) determination, which is essential for the improvement of the theory of the motion of artificial satellites like TOPEX/Poseidon or ENVISAT and for orbit determination of uncooperative targets like rocket bodies from the LEO regime. The information about the position and behaviour in space of targets like TOPEX/Poseidon and ENVISAT is very important from the point of view of future debris removal missions. Not only the exact knowledge on the position of the defunct satellite/space debris is needed but also the precise information about its rotation/tumbling and orientation in space is required. Figure 39 presents sample results for the Ocean Topography Experiment (TOPEX/Poseidon) satellite.

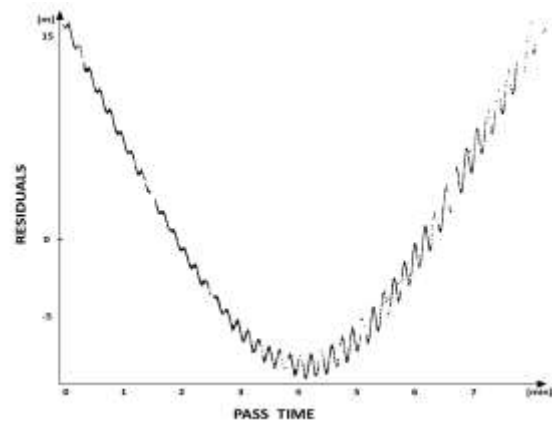


Fig. 39 Pass of TOPEX/Poseidon over BORL station on 27 January 2017 at 03:46 UTC (2 614 returns and RMS is 38.37 cm)

This is a defunct satellite that was orbiting in an uncontrolled way since 2005. The TOPEX/Poseidon mission is one of the most successful missions prepared by NASA and the Centre National d'Études Spatiales (CNES). The spacecraft launched on 10 August 1992 is huge (11.5 m × 5.5 m × 6.6 m) of a mass over 2 tons. It orbits at the altitude of about 1300 km. The satellite is equipped with an annulus RRA (retroreflector array) with 192 corner cubes. The pass duration over the station is maximum 12 minutes. The main objectives of TOPEX/Poseidon included:

- monitoring of global ocean circulation,
- climate change studies,
- monitoring of the Earth's atmosphere.

On 9 October 2005, control stabilisation was lost and the satellite started to rotate. Currently TOPEX/Poseidon is spinning at about 10 s/rev and is in the accelerating mode. As in the case of ENVISAT and JASON-1, the laser observations of TOPEX/Poseidon are used mainly for studies of satellite/space debris spin dynamics (Kucharski et al., 2017).

In Figure 40 sample results from ENVISAT are shown. This spacecraft, which belongs to the ESA, was launched on 1 March 2002. ENVISAT was assigned for remote sensing and environmental monitoring. It was one of the most successful missions in the ESA's history. Like TOPEX/Poseidon, this spacecraft was orbiting in an uncontrolled way since 2012. It is particularly huge (26 m × 10 m × 5 m) and massive (over 8 tons).

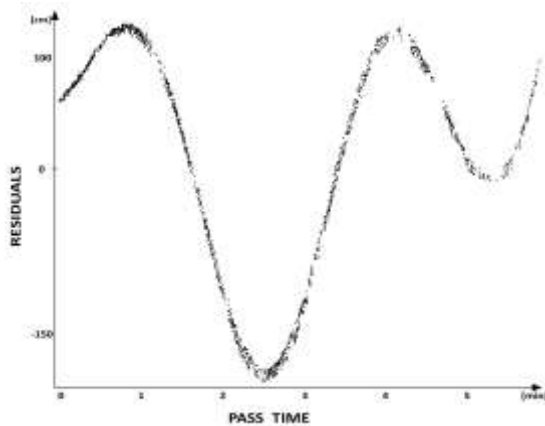


Fig. 40 Pass of ENVISAT over BORL station on 28 March 2017 at 19:30 UTC (1759 returns and RMS is 3.61 cm)

In 2017 the activity of the BORL station was focused on the Space Surveillance and Tracking (SST) programme, which constitutes one of the pillars of the Space Situational Awareness (SSA) programme carried out by the ESA and the EC. The SST programme is dedicated to monitoring (observing and detecting) for active and inactive satellites, discarded launch stages and fragmentation debris orbiting the Earth. The activity of the BORL station in the SST includes research and development in satellite laser ranging. In the middle of 2017 Poland applied to the EU SST Consortium (Application of the Republic of Poland to participate in the Space Surveillance and Tracking Support Framework Decision No 541/2014/EU of the European Parliament and the Council). The SRC PAS is one of the members of the Polish SST consortium (Konacki et al., 2017).

At Borowiec Observatory, a second independent laser system is under development. This system is dedicated to the SST programme. The new system is situated on an azimuth-elevation mount with a 65 cm Cassegrain telescope (Fig. 41) equipped with servo drives that provide tracking accuracy below 1 arcsec, and a 20 cm Maksutov guiding telescope equipped with two fast dedicated optical CMOS cameras.

The whole system is controlled by a multiplatform steering/tracking software (Fig. 42) and will support space debris/satellite prediction, real-time laser observations, system calibration, ADSB monitoring, data post-processing and other

functions. The system will operate 24 hours a day, 7 days a week. Currently, the new telescope mount is in tracking mode.



Fig. 41. Second independent satellite laser system developed by SRC PAS (main telescope)



Fig. 42. Second independent satellite laser system developed by SRC PAS (operator room)

## 11. Geodynamics

IGiK, WAT and WUELS, integrated into the GGOS-PL network, together with the Institute of Geophysics of the Polish Academy of Sciences and with some other institutions started at the beginning of 2017 a common geodynamics research in the framework of the European Plate Observing System Programme (EPOS). EPOS-PL project – the Polish Earth science infrastructure integrated with the EPOS programme (Bosy et al., 2017). In particular, activities on developing centres of research infrastructure for geomagnetic and gravimetric data integrated with GNSS infrastructure (Sosnica et al., 2017) was initiated.

Simultaneous seismic and gravity records at the same locations allow the study of a wider response for incoming seismic waves by using two quite different instruments and in consequence the structure of the lithosphere. For test purposes 4 seismometer-gravimeter pairs were temporarily deployed in Poland at three locations: Borowa Gora Geodetic-Geophysical Observatory (BG), Jozefoslaw Astro-Geodetic Observatory (JO), and

Lamkowko Satellite Observatory (LA). During the test period from December 2016 to May 2017 several large teleseismic events were observed with well-formed surface waves (Dykowski et al., 2017a). The correlation of a broadband seismometer signal with different types of gravimetric sensors signals the opportunity to analyse gravimeter noise components, in the instrumental and micro-seismic domains. The superconducting gravimeter iGrav-027 shows excellent consistency with the seismometer within the frequency range of a seismometer (up to 120 s periods) (Fig. 43).

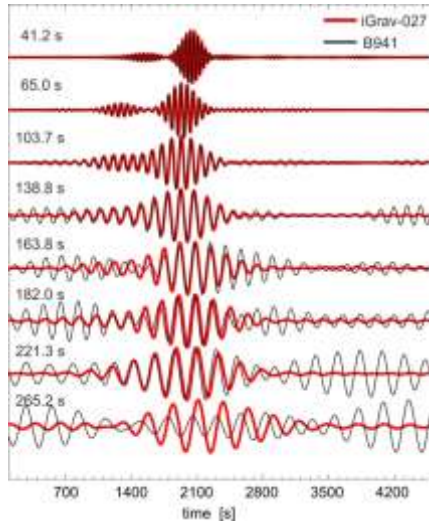


Fig. 43. Near monochromatic complex signal of the M6.6 Kamchatka earthquake recorded by the B941 seismometer (thin black line) and the iGrav-027 superconducting gravimeter (red line) at the Borowa Gora Observatory

Spring gravimeters also proved good consistency with the seismometer, yet their recordings need further analysis (Wilde-Piorko et al., 2017).

Research on the developing the integrated system of surface deformation monitoring caused by man-made factors, based on Persistent Scatterer Interferometry, measurements from permanent GNSS stations and precise levelling has been continued in IGiK in cooperation with two other institutions.

The results obtained in a case study for Poland performed by the team of IGiK (Godah et al. 2017d) reveal that the combination of temporal geoid height variations and temporal vertical displacements of the physical surface of the Earth result in significant temporal variations of the vertical reference system for the area investigated. Taking into the consideration the dispersion (i.e. maximum – minimum) ratio of 1:1.15 between temporal variations of geoid height and temporal vertical displacement, temporal variations of orthometric/normal heights over the area of Poland may reach up to 2.4 cm from epoch to epoch. In the Borowa Gora Observatory for the period from

01/2004 to 12/2006 it reaches up to 1.6 cm (Fig. 44).

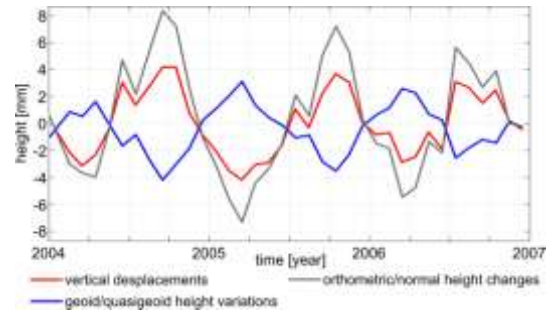


Fig. 44. Temporal vertical displacements, temporal variations of geoid height and temporal variations of the orthometric/normal height at the Borowa Gora Observatory

PSI and GNSS results were jointly processed recreating the history of surface deformation of the area of Warsaw metropolitan with the use of radar images from Cosmo SkyMed, TerraSAR-X, and Sentinel-1 satellites (Krynski et al., 2017a, 2017b). GNSS data from Borowa Gora and Jozefoslaw observatories as well as from WAT1 and CBKA permanent GNSS stations were used to validate the obtained results. Observations from 2000-2016 were processed with the Bernese v.5.0 software. Relative height changes between the GNSS stations were determined from GNSS data and relative height changes between the persistent scatterers located on the objects with GNSS stations were determined from the interferometric results. The consistency of results of the two methods was 3 to 4 times better than the theoretical accuracy of each. The joint use of both methods allows to extract a very small height change below the level of measurement error. Relative deformations in height component between GNSS stations obtained from GNSS (weekly solutions) and PSI (average) Cosmo SkyMed, TerraSAR-X, and Sentinel-1 data were compared (Fig. 45).

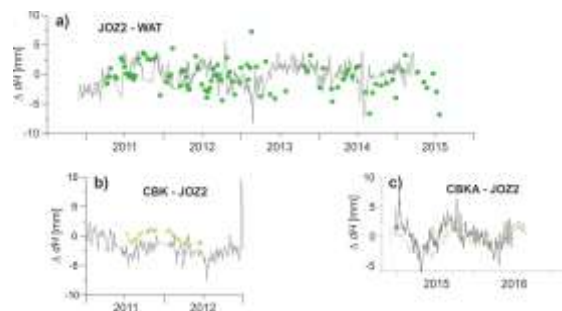


Fig. 45. Relative deformations in height component obtained from GNSS (weekly solutions) and PSI (average) data: Cosmo SkyMed (a), TerraSAR-X (b), and Sentinel-1 (c)

It has been proved that the use of mutually complementing observation techniques for monitoring deformations in the investigated area, such as GNSS and PSI, can substantially increase

reliability of the interpretation of the results obtained. It should be expected that comparing the results of the GNSS data with PSI data of higher spatial resolution, and in particular of higher temporal resolution, e.g. Cosmo-SkyMed or Sentinel-1 data, should give better results and allow to extract larger signal of height changes from the observed variations of vertical component of the GNSS station.

## Acknowledgements

The following researchers submitted data used to elaborate this report: Andrzej Araszkiwicz, Monika Biryło, Andrzej Borkowski, Jarosław Bosa, Przemysław Dykowski, Mariusz Figurski, Tomasz Hadaś, Paweł Hordyniec, Grzegorz Józków, Jan Kapłon, Kamil Kazmierski, Michał Kruczyk, Jan Kryński, Paweł Lejba, Tomasz Liwosz, Adam Lyszkowicz, Jolanta Nastula, Grzegorz Nykiel, Tomasz Olszak, Jerzy Rogowski, Witold Rohm, Jan Sierny, Jarosław Somla, Krzysztof Sońnica, Janusz Walo, Paweł Wielgosz, Monika Wilde-Piórko, Karina Wilgan.

## References

- Baldysz Z., Szolucha M., Nykiel G., Figurski M., (2017): *Analysis of the Impact of Galileo Observations on the Tropospheric Delays Estimation*, 2017 Baltic Geodetic Congress (BGC Geomatics), Gdansk, Poland, pp. 65–71, DOI: 10.1109/BGC.Geomatics.2017.22
- Baldysz Z., Nykiel G., Figurski M., Araszkiwicz A., (2018): *Assessment of the Impact of GNSS Processing Strategies on the Long-Term Parameters of 20 Years IWW Time Series*, Remote Sensing, 10(4), 496, doi:10.3390/rs10040496
- Banville S., Sieradzki R., Hoque M., et al., (2017): *On the estimation of higher-order ionospheric effects in precise point positioning*, GPS Solutions 21, Issue 4, pp. 1817–1828, <https://doi.org/10.1007/s10291-017-0655-0>
- Biryło M., Rzepecka Z., Kuczynska-Siehien J., Nastula J., (2017): *Analysis of water budget prediction accuracy using Arima models*, Water Science and Technology: Water Supply Journal, Vol. 18, Issue 1, DOI: 10.2166/ws.2017.156.
- Bernatowicz A., Lyszkowicz A., (2017): *Present state of lake studies from satellite altimetry – a case study in Poland*, “Environmental Engineering” 10<sup>th</sup> International Conference eISSN 2029-7092 / eISBN 978-609-476-044-0 Vilnius Gediminas Technical University, Lithuania, 27–28 April 2017, pp. 1–8, <https://doi.org/10.3846/enviro.2017.164> (15)
- Biryło M., (2017a): *Uncertainty in estimated water cycle determined with atmospheric budget, water budget and total water storage*, European Waters, Vol. 59, E.W. Publications.
- Biryło M., (2017b): *Evaluation of the water cycle determined with atmospheric and water budgets and total water storage*, Water Resources Management, Springer (under review).
- Bobkowska K., Nykiel G., Tysiac P., (2017): *DMI measurements impact on a position estimation with lack of GNSS signals during Mobile Mapping*, IOP Conf. Series: Journal of Physics: Conf. Series 870 012010 doi:10.1088/1742-6596/870/1/012010
- Bosa J., Orlecka-Sikora B., Olszewska D., Górka-Kostrubiec B., Lizurek G., Lurka A., Jóźwiak W., Welker E., Werner T., Junosza-Szaniawski R., Araszkiwicz A., Kaplon J., Kryński J., Dykowski P., Czuba W., Janik., Sońnica K., Rohm W., Tymków P., Borkowski A., Hadaś T., Mutke G., Barański A., Szepieniec T., Kocot J., (2017): *EPOS – PL the initiative for European Plate Observation System in Poland, integrated infrastructure and new algorithms*, Symposium of the IAG Subcommission for Europe (EUREF) held in Wrocław, Poland, 17–19 May 2017 <http://www.euref.eu/symposia/2017Wroclaw/04-04-Bosa.pdf>.
- Calka B., Bielecka E., Figurski M., (2017): *Spatial pattern of ASG-EUPOS sites*, Open Geosciences, 9(1), pp. 613–621, doi:10.1515/geo-2017-0046
- Ding W., Teferle F.N., Kazmierski K., Laurichesse D., Yuan Y., (2017): *An evaluation of real-time troposphere estimation based on GNSS Precise Point Positioning*, Journal of Geoph. Res.: Atmospheres, 122(5), pp. 2779–2790.
- Dykowski P., Kryński J., (2017): *Aspects of establishing a modern gravity control: case study Borowa Gora Observatory*, Symposium of the IAG Subcommission for Europe (EUREF) held in Wrocław, Poland, 17–19 May 2017, <http://www.euref.eu/symposia/2017Wroclaw/p-14-Dykowski.pdf>.
- Dykowski P., Grad M., Krankowski A., Krynski J., Olszak T., Polkowski M., Rajner M., Sekowski M., Wilde-Piórko M., (2017a): *Expanding seismic surface waves measurements towards low periods with gravity measurements*, IAG-IASPEI Scientific Assembly, Kobe, Japan, 30 July – 4 August 2017.
- Dykowski P., Sękowski M., Kryński J., (2017b): *First year of gravity signal records with the iGrav-027 superconducting gravimeter*, IAG-IASPEI Scientific Assembly, Kobe, Japan, 30 July – 4 August 2017.
- Figurski M., Nykiel G., (2017): *Investigation of the impact of ITRF2014/IGS14 on the positions of the reference stations in Europe*, Acta Geodyn. Geomater., Vol. 14, No 4(188), pp. 401–410, doi: 10.13168/AGG.2017.0021
- Godah W., Szelachowska M., Krynski J., (2017a): *Application of the PCA/EOF method for the analysis and modelling of temporal variations of geoid heights over Poland*, Acta Geodaetica et Geophysica, Vol. 53, Issue 1, pp. 93–105, DOI 10.1007/s40328-017-0206-8, <https://link.springer.com/article/10.1007/s40328-017-0206-8>
- Godah W., Szelachowska M., Krynski J., (2017b): *On the estimation of physical height changes using GRACE satellite mission data – A case study of Central Europe*, Symposium of the IAG Subcommission for Europe (EUREF) held in Wrocław, Poland, 17–19 May 2017 <http://www.euref.eu/symposia/2017Wroclaw/02-10-Godah.pdf>; Geodesy and Cartography, Vol. 66, No 21, pp. 213–228, DOI: 10.1515/geocart-2017-0013
- Godah W., Szelachowska M., Krynski J., (2017c): *On the analysis of temporal geoid height variations obtained from GRACE-based GGMs over the area of Poland*, Acta Geophysica, pp. 713–725. <https://doi.org/10.1007/s11600-017-0064-3>
- Godah W., Szelachowska M., Krynski J., (2017d): *Investigation of geoid height variations and vertical displacements of the Earth surface in the context of the realization of the modern vertical reference system – A case study for Poland*. IAG Symposia, Springer, Berlin, Heidelberg, [https://doi.org/10.1007/1345\\_2017\\_15](https://doi.org/10.1007/1345_2017_15)
- Godah W., Krynski J., Szelachowska M., (2018): *The use of absolute gravity data for the validation of Global Geopotential Models and for improving quasigeoid heights determined from satellite-only Global Geopotential Models*, Journal of Applied Geophysics,

- Vol. 152, May 2018, pp. 38–47, doi:10.1016/j.jappgeo.2018.03.002.
- Golaszewski P., Stepniak K., Wielgosz P., (2017): *Zenith Tropospheric Delay Estimates Using Absolute and Relative Approaches to GNSS Data Processing – Preliminary Results*, 2017 Baltic Geodetic Congress (BGC Geomatics), Gdansk, 2017, pp. 414–418, DOI: 10.1109/BGC.Geomatics.2017.79
- Hadas T., Krypiak-Gregorzcyk A., Hernández-Pajares M., Kaplon J., Paziewski J., Wielgosz P., Garcia-Rigo A., Kazmierski K., Sosnica K., Kwasniak D., Sierny J., Bosy J., Pucilowski M., Szyszko R., Portasiak K., Olivares-Pulido G., Gulyaeva T., Orus-Perez R., (2017a): *Impact and implementation of higher-order ionospheric effects on precise GNSS applications*, Journal of Geophysical Research: Solid Earth, 122, <https://doi.org/10.1002/2017JB014750>
- Hadaś T., Teferle F.N., Kaźmierski K., Hordyniec P., Bosy J., (2017b): *Optimum stochastic modeling for GNSS tropospheric delay estimation in real-time*, GPS Solutions, Vol. 21, No 3, Berlin – Heidelberg 2017, pp. 1069–1081, DOI: 10.1007/s10291-016-0595-0
- Hernández-Pajares M., Wielgosz P., Paziewski J., Krypiak-Gregorzcyk A., Krukowska M., Stepniak K., Kaplon J., Hadas T., Sosnica K., Bosy J., Orus-Perez R., Monte-Moreno E., Yang H., Garcia-Rigo A., Olivares-Pulido G., (2017): *Direct MSTID mitigation in precise GPS processing*, Radio Science, Vol. 52, No 3, pp. 321–337, DOI: 10.1002/2016RS006159
- Kačmařík M., Douša J., Dick G., Zus F., Brenot H., Möller G., Pottiaux E., Kaplon J., Hordyniec P., Václavovic P., Morel L., (2017): *Inter-technique validation of tropospheric slant total delays*, Atmos. Meas. Tech., 10, 2183–2208, <https://doi.org/10.5194/amt-10-2183-2017>
- Kazmierski K., Santos M., Bosy J., (2017): *Tropospheric delay modelling for the EGNOS augmentation system*, Survey Review, 49(357), pp. 399–407.
- Konacki M., Lejba P., Sybilski P., Pawłaszek R., Kozłowski S., Suchodolski T., Słonina M., Litwicki M., Sybilska A., Rogowska B., Kolb U., Burwitz V., Baader J., Groot P., Bloemen S., Ratajczak M., Helminiak K., Borek R., Chodosiewicz P., Chimicz A., (2017): *The Solaris-Panoptes Global Network of Robotic Telescopes and the Borowiec Satellite Laser Ranging System for SST: A Progress Report*, Proc. of the Advanced Maui Optical and Space Surveillance Technologies (AMOS) Conference, AMOS 2017, <http://amostech.com/2017-technical-papers/>
- Kruczyk M., Liwosz T., Pietruczuk A., (2017): *Integrated precipitable water from GPS observations and CIMEL sunphotometer measurements at CGO Belsk*, Reports on Geodesy and Geoinformatics, No 103/2017, pp. 46–65, DOI:10.1515/rgg-2017-0005
- Krynski J., Rogowski J.B., (2017): *National Report of Poland to EUREF 2017*, Symposium of the IAG Subcommission for Europe (EUREF) held in Wrocław, Poland, 17–19 May 2017 <http://www.euref.eu/symposia/2017Wroclaw/05-17-p-Poland.pdf>
- Krynski J., Zak L., Ziolkowski D., Cisak J., Lagiewska M., (2017a): *Estimation of height changes of GNSS stations from the solutions of short vectors and PSI measurements*, Geodesy and Cartography, Vol. 66, No 1, pp. 73–88, DOI: 10.1515/geocart-2017-0008
- Krynski J., Zak L., Ziolkowski D., Lagiewska M., Cisak J., (2017b): *Joint estimate of height changes from GNSS solutions of short vectors and PSI measurements using Envisat and TerraSAR-X satellite data*, Symposium of the IAG Subcommission for Europe (EUREF) held in Wrocław, Poland, 17–19 May 2017 <http://www.euref.eu/symposia/2017Wroclaw/p-11-Krynski.pdf>
- Kucharski D., Kirchner G., Bennett J.C., Lachut M., Sośnica K., Koshkin N., Shakun L., Koidl F., Steindorfer M., Wang P., Fan C., Han X., Grunwaldt L., Wilkinson M., Rodriguez J., Bianco G., Vespe F., Catalán M., Salmins K., del Pino J.R., Lim H.-C., Park E., Moore C., Lejba P., Suchodolski T., (2017): *Photon pressure force on space debris TOPEX/Poseidon measured by Satellite Laser Ranging*, Earth and Space Science, Vol. 4, Issue 10, pp. 661–668, October, 2017.
- Kuczynska-Siehien J., Lyszkowicz A., (2017): *Evaluation of the altimetry data in the Baltic Sea region and computation of the new quasigeoid models for Poland*, IAG-IASPEI Scientific Assembly, Kobe, Japan, 30 July – 4 August 2017.
- Liwosz T., (2015): *Report of the WUT Analysis Centre*, EUREF Local Analysis Centres Workshop, 14–15 October, Bern, Switzerland, [http://www.epncb.oma.be/newseventslinks/workshops/EPNLACWS\\_2015/pdf/report\\_of\\_the\\_WUT\\_analysis\\_centre.pdf](http://www.epncb.oma.be/newseventslinks/workshops/EPNLACWS_2015/pdf/report_of_the_WUT_analysis_centre.pdf)
- Liwosz T., Araszkievicz A., (2017): *EPN Analysis Coordinator Status Report*, Symposium of the IAG Subcommission for Europe (EUREF) held in Wrocław, Poland, 17–19 May 2017, <http://www.euref.eu/symposia/2017Wroclaw/02-01-Liwosz.pdf>
- Lyszkowicz A., Bernatowicz A., (2017): *Current state of art of satellite altimetry*, Geodesy and Cartography, Vol. 66, No 2, pp. 265–276, DOI: 10.1515/geocart-2017-0016
- Malyszko L., Paziewski J., Sieradzki R., Kowalska E., Rutkiewicz A., (2017): *Detecting Cantilever Beam Vibration with Accelerometers and GNSS*, 2017 Baltic Geodetic Congress (BGC Geomatics), Gdansk, 2017, pp. 148–152, doi: 10.1109/BGC.Geomatics.2017.10
- Nykiel G., Figurski M., (2017): *Impact of Galileo Observations on the Position and Ambiguities Estimation of GNSS Reference Stations*, 2017 Baltic Geodetic Congress (BGC Geomatics), Gdansk, Poland, pp. 225–231, DOI: 10.1109/BGC.Geomatics.20.17.11
- Nykiel G., Zanimonskiy Y.M., Yampolski Y.M., Figurski M., (2017): *Efficient Usage of Dense GNSS Networks in Central Europe for the Visualization and Investigation of Ionospheric TEC Variations*, Sensors, 17(10):2298, DOI: 10.3390/s17102298
- Nykiel G., Wolak P., Figurski M., (2018): *Atmospheric opacity estimation based on IWV derived from GNSS observations for VLBI applications*, GPS Solutions, 22:9, DOI: 10.1007/s10291-017-0675-9
- Olszak T., Barlik M., Pachuta A., (2017): *Hydrogeologiczne przyczyny zmian przyspieszenia siły ciężkości na stanowisku w Obserwatorium Astronomiczno-Geodezyjnym w Józefosławiu*, Przegląd Geologiczny, Vol. 65, No 11/1, pp. 1139–1143.
- Pálínkás V., Francis O., Val'ko M., Kostelecký J., Van Camp M., Castelein S., Bilker-Koivula M., Näränen J., Lothhammer A., Falk R., Schilling M., Timmen L., Iacovone D., Baccaro F., Germak A., Biolcati E., Origlia C., Greco F., Pistorio A., de Plaen R., Klein G., Seil, Radinovic R., Reudink R., Dykowski P., Sękowski M., Próchniewicz D., Szpunar R., Mojżeś M., Jańak J., Papčo J., Engfeldt A., Olsson P.A., Smith V., van Westrum D., Ellis B., Lucero B., (2017): *Regional comparison of absolute gravimeters, EURAMET.M.G-K2 key comparison*, Metrologia 54, DOI:10.1088/0026-1394/54/1A/07012.
- Paziewski J., Wielgosz P., (2017): *Investigation of some selected strategies for multi-GNSS instantaneous RTK positioning*, Advances in Space Research, Vol. 59(1), pp. 12–23, DOI 10.1016/j.asr.2016.08.034
- Paziewski J., Sieradzki R., (2017): *Integrated GPS+BDS instantaneous medium baseline RTK positioning: signal analysis, methodology and performance assessment*,

- Advances in Space Research, DOI 10.1016/j.asr.2017.04.016
- Paziewski J., Sieradzki R., Baryła R., (2017): *High-rate GNSS positioning for precise detection of dynamic displacements and deformations: methodology and case study results*, In: "Environmental Engineering" 10<sup>th</sup> International Conference Vilnius Gediminas Technical University, Lithuania, 27–28 April 2017, DOI: <https://doi.org/10.3846/enviro.2017.224>
- Rzepecka Z., Birylo M., Kuczynska-Sieghien J., Nastula J., Pajak K., (2017): *Analysis of groundwater level variations and water balance In the area of the Sudety Mountains*, Acta Geodynamica et Geomaterialia, Vol. 14, No 3(187), pp. 307–315, DOI: 10.13168/AGG.2017.0014
- Sośnica K., Bosy J., Kaplon J., Rohm W., Hadaś T., Sierny J., Kudłacik I., Zajdel R., Kryński J., Dykowski P., Araszkiewicz A., Mutke G., Kotyrba A., Olszewska D., (2017): *Densification of the GGOS infrastructure in Poland in the framework of EPOS-PL*, Symposium of the IAG Subcommission for Europe (EUREF) held in Wrocław, Poland, 17–19 May 2017, <http://www.euref.eu/symposia/2017Wroclaw/04-03-Sosnica.pdf>.
- Stepniak K., Baryła R., Paziewski J., Golaszewski P., Wielgosz P., Kurpinski G., Osada E., (2017): *Validation of regional geoid models for Poland: Lower Silesia case study*, Acta Geodynamica et Geomaterialia, Vol. 14, No 1(185), pp. 93–100, DOI: 10.13168/AGG.2016.0031
- Stepniak K., Bock O., Wielgosz P., (2018): *Reduction of ZTD outliers through improved GNSS data processing and screening strategies*, Atmos. Meas. Tech., 11, pp. 1347–1361, <https://doi.org/10.5194/amt-11-1347-2018>
- Toth C., Jozkow G., Koppanyi Z., Grejner-Brzezinska D., (2017): *Positioning Slow-Moving Platforms by UWB Technology in GPS-Challenged Areas*, J. Surv. Eng., 143(4), 04017011.
- Welker E., Reda J., Pałka A. (2017): *Magnetic repeat station network on the Baltic Sea – why so needed?*, Annual of Navigation, 24/2017, pp. 19–30.
- Wilde-Piorko M., Dykowski P., Polkowski M., Olszak T., Grad M., Krynski J., Sekowski M., Krankowski A., Rajner M., (2017): *Expanding seismic surface waves measurements towards low periods with gravity measurements*, Geoinformation Issues, Vol. 9, No 1(9), pp. 5–13.
- Wilgan K., Hadaś T., Hordyniec P., Bosy J., (2017): *Real-time precise point positioning augmented with high-resolution numerical weather prediction model*, GPS Solutions, Vol. 23 No 3, Berlin - Heidelberg 2017, pp. 1341–1353, DOI: 10.1007/s10291-017-0617-6
- Winska M., Nastula J., Salstein D., (2017): *Hydrological excitation of polar motion by different variables from the GLDAS models*, Journal of Geodesy, 91(12), pp. 1461–1473, <https://doi.org/10.1007/s00190-017-1036-8>
- Zanimonskiy Y.M., Dudnik O.V., Nykiel G., Figurski M., (2017): *Investigation of some magnetospheric phenomena of geomagnetic storm on March 17, 2013 based on observations from GNSS and NOAA-15 satellite*, Proc. of 6<sup>th</sup> International Radio Electronic Forum (IREF2017). International Scientific Conference "Radars. Satellite navigation. Radiomonitoring", Kharkiv, Ukraine, 24–26 October, 2017, pp. 196–199. [www.asgeupos.pl](http://www.asgeupos.pl)